(12)

AFGL-TR-82-0057

ABSORPTION MEASUREMENTS OF CO_2 AND H_2O AT HIGH RESOLUTION AND ELEVATED TEMPERATURES

Mark P. Esplin
Ronald J. Huppi
Hajime Sakai
George A. Vanasse
Laurence S. Rothman

Electro-Dynamics Laboratories (SRL)
Utah State University
139 The Great Road
Bedford, Massachusetts 01730

Scientific Report No. 1

February 1982

Approved for public release; distribution unlimited

AIR FORCE GEOPHYSICS LABORATORY
AIR FORCE SYSTEMS COMMAND
UNITED STATES AIR FORCE
HANSCOM AFB, MASSACHUSETTS 01731

Unclassified

SECURITY CLASSIFICATION OF THIS PAGE (When Data Entered)

REPORT DOCUMENTATION PAGE

READ INSTRUCTIONS BEFORE COMPLETING FORM

1. REPORT NUMBER: AFGL-TR-82-0057	2. GOVT ACCESSION NO.: AD-A113 824
3. RECIPIENT'S CATALOG NUMBER: EDL-SRL-82-1	
4. TITLE (and Subtitle): Absorption Measurements of CO_2 and H_2O at High Resolution and Elevated Temperatures	5. TYPE OF REPORT & PERIOD COVERED: Scientific Report No. 1
	6. PERFORMING ORG. REPORT NUMBER
7. AUTHOR(s): Mark P. Esplin, Ronald J. Huppi, Hajime Sakai*, George A. Vanasse** and Laurence S. Rothman**	8. CONTRACT OR GRANT NUMBER(s): F19628-81-C-0113
9. PERFORMING ORGANIZATION NAME AND ADDRESS: Electro-Dynamics Laboratories (SRL), Utah State University, 139 The Great Road, Bedford, MA 01730	10. PROGRAM ELEMENT, PROJECT, TASK AREA & WORK UNIT NUMBERS: 61102F, 2310G1AR
11. CONTROLLING OFFICE NAME AND ADDRESS: Air Force Geophysics Laboratory, Hanscom AFB, Massachusetts 01731, Monitor: Dean Kimball OPR	12. REPORT DATE: February 1982
	13. NUMBER OF PAGES: 97
14. MONITORING AGENCY NAME & ADDRESS (if different from Controlling Office)	15. SECURITY CLASS. (of this report): Unclassified
	15a. DECLASSIFICATION/DOWNGRADING SCHEDULE

16. DISTRIBUTION STATEMENT (of this Report)

Approved for public release; Distribution unlimited.

17. DISTRIBUTION STATEMENT (of the abstract entered in Block 20, if different from Report)

18. SUPPLEMENTARY NOTES

This research was supported by the Air Force Office of Scientific Research.
*University of Mass., Amherst, MA
**AFGL, Hanscom AFB, Massachusetts 01731

19. KEY WORDS (Continue on reverse side if necessary and identify by block number)

CO_2, H_2O, spectroscopic constants, interferometer, high resolution, high temperature

20. ABSTRACT (Continue on reverse side if necessary and identify by block number)

High resolution (0.007 cm^{-1}) high temperature (to 800K) measurements of H_2O and several isotopes of CO_2 using the AFGL high resolution cat's eye interferometer are presented. The instrumentation used is briefly described and resulting line positions used to obtain spectroscopic constants are tabulated. A general description of the technique used for identifying transition frequencies is given as well as its specific application to the H_2O and CO_2 molecules. Comparisons of calculations of line positions using

DD FORM 1 JAN 73 1473

Unclassified

SECURITY CLASSIFICATION OF THIS PAGE (When Data Entered)

20. Abstract (Continued)

spectroscopic constants obtained from high temperature data with those obtained at room temperature are presented. A global fit approach to the CO_2 data is also discussed, incorporating high resolution measurements throughout the infrared to achieve a self-consistent set of spectroscopic constants.

Acknowledgement

The measurements and analysis presented in this report were supported by the Air Force Office of Scientific Research under Grant AFOSR 78-3702, Project 2301, the Atmospheric Sciences Project 2310 and performed as part of AFGL Task 2310G1, IHWUs 2310G101 and 2310G106 and also under AFGL Contract F19628-81-C-0113. We would like to acknowledge Mr. William Dalton and Mrs. Shui-Hua Li from the University of Massachusetts and Mr. Vaughn Griffiths of the Stewart Radiance Laboratory of Utah State University for their help in obtaining the data.

Table of Contents

List of Figures

List of Figures (Continued)

List of Tables

I. INTRODUCTION

The molecular species CO_2 and H_2O are major atmospheric constituents which critically control the infrared radiative transfer in the earth's atmosphere. Their absorption bands are distributed over a wide spectral range, extending from the near to the far infrared region of the electromagnetic spectrum. These species have been extensively studied since infrared spectroscopy technology came into existence; however, there are still gaps in our knowledge of the infrared absorption of these two molecules. In particular, our understanding of their absorption at high temperatures remains incomplete. The bands observable at room temperature are restricted to transitions which originate from a lower state of a relatively small excitation energy—typically from a vibrational-rotational energy below 2000 cm^{-1}. Transitions at room temperature are weak since these lower states are insufficiently populated. They cannot be studied well even with measurements through extremely long absorption paths. These are the transitions which originate from lower states of high vibrational-rotational energy and become observable when the gas temperature is raised to increase their population density. These transitions, generally referred to as the hot bands, are poorly known because of the paucity of measurements.

Various experimental difficulties are encountered in the spectroscopic measurement of gases at elevated temperatures. The original AFGL compilation of the atmospheric line parameters

was assembled primarily for application to room temperature calculations. The basic line parameters were derived from room temperature data. Consequently, the accuracy which the data provided was generally unsuitable for spectral synthesis calculation for high temperatures. The line parameters compiled for the hot bands of these molecules do not provide an accuracy sufficient for line position extrapolation to high temperature. The present experimental effort was begun with the intent to solve this difficulty by measuring the absorption of these molecules at elevated temperatures and obtaining improved line parameters which could yield more accurate results in spectral syntheses at high temperatures and high resolution.

The excitation which occurs in a heated gas maintains thermal equilibrium of the molecular system; the distribution, or population as a function of energy level, is controlled by the Boltzmann factor $e^{-E/kT}$, where E is the vibrational-rotational energy of the state in question. There would be no preferential excitations among various vibrational levels. If two states which belong to two different vibrational states have a similar energy, $E_1 \approx E_2$, both states are excited at an equal rate. A marked increase in the observable transitions consequently occurs along two directions as the temperature of the molecular system is increased; there is a marked increase in observable vibrational transitions as well as in rotational transitions within a vibrational transition.

The spectral structure consequently increases in complexity as the gas temperature is raised.

The increased complexity in the spectra poses two problems: one is a requirement for increased spectral resolution, and another is for the identification of the individual spectral transitions. The spectra must be observed with adequate spectral resolution for the isolation of most of the transitions of interest. The spectral coverage must be broadened since more rotational lines are excited within a vibrational band. The problem of spectrometry is, for our case, adequately solved by use of the technique of Fourier spectroscopy. The second problem concerning identification of the observed spectral transitions was found more difficult than expected. To overcome this difficulty the spectral data were taken at temperature steps of 200K, i.e., at 600K and at 800K. We hoped to follow the excitation of the hot bands in the data taken at these temperatures. For the H_2O data, the temperature step taken was adequate, while it was found inadequate for the CO_2 data. The increase in observable CO_2 lines from 600K to 800K was overwhelming; at 600K we were able to make the assignment of the observed CO_2 lines without encountering serious difficulty, while at 800K an automated Loomis-Wood diagram technique was developed for the purpose of simplifying the identification.

An absorption cell which could be operated at elevated temperatures was designed and constructed. The instrumentation

problem was mainly a question of stability in the optical path during high temperature operation. Prior experience indicated that the White cell configuration was totally inadequate for high temperature operation and that a Pfund cell configuration might work very well. Even so, the multipass optical system was found difficult to operate at high temperature - it worked within a limited temperature range. The mirror surface coated with a Rh film was adequate for the measurements at 600K and 800K. The cell transmission was found to deteriorate rapidly as the temperature was raised above 1000K. A single-pass optical configuration which required no mirror optics seemed the only arrangement with promise of successful operation at temperatures above 1000K.

The measurements consisted of obtaining absorption data of both gases at two temperatures, 600K and 800K in the spectral region between 1600 to 2500 cm^{-1}. Analysis of the CO_2 data clearly indicated that a high accuracy of the measurement of the line positions is inadequate for extrapolating to the highest rotational transitions. The vibrational-rotational transitions of a linear polyatomic molecule (for example the Q branch) can be given by the simple expression:

$$\sigma(J) = G' + B' J'(J'+1) - D'[J'(J'+1)]^2 + H'[J'(J'+1)]^3$$
$$- G'' - B'' J''(J''+1) + D''[J''(J''+1)]^2 - H''[J''(J''+1)]^3.$$

It was found that the parameters, B, D, and H, determined from the measurement had a meaningful accuracy only within the

measured transition range. They were by no means effective in predicting the transitions outside the range. For example, we found that those parameters determined from the data between P(50) to R(50) with high accuracy could predict P(60) to R(60) lines to poor accuracy.

The intensities of the CO_2 lines observed in the data were not determined absolutely. In complex spectra such as those reported on here, very few observed spectral features are composed of single transitions. In dealing with the complex data we must determine the individual line intensities simultaneously for multiline components. The assignment of the exact positions for the component lines is of crucial importance to the effort. Because of this, the identification of all transitions observed in the data is of prime importance for the data analysis. An extended effort is required for the assignment of transitions.

The H_2O data contrasted in many ways with the CO_2 data. The H_2O molecule is an asymmetric top rotor; the rotational lines are distributed in a manner not so simple as a linear molecule and its vibrational frequencies are much larger than those of CO_2. Even though the H_2O spectrum contains far less lines than the CO_2 spectrum, its structure is far more complex than the latter. Nevertheless the analysis went well. The identifications of the transitions for H_2O and CO_2 and the intensities for H_2O were made using the 600K and 800K data.

II. GENERAL CONSIDERATIONS

In all our observed spectra the 100% transmittance level was not constant but varied as a function of wavenumber. This variation was due to several factors such as, a variation in detector spectral sensitivity, the spectral transmission characteristics of the bandpass filter and probably of the interferometer as well. By far the most bothersome background level modulation was caused by the light interference between various optical surfaces which the infrared beam traversed. The molecular absorptance (for the case of H_2O) was determined with respect to the non-uniform 100% transmission level and, in spite of using various computation logics to reduce the effect of the background uncertainty, the uncertainty in the absorption was still greater than 5%.

The absorption spectra, determined as indicated above, were then analyzed to obtain transition frequencies. Since the computer output is a spectrum consisting of discrete values in wavenumber at an interval corresponding to the reciprocal of twice the maximum path difference in the interferogram, it is not smooth enough for analysis, i.e., connecting the spectral output points by straight lines results in a very jagged spectrum. It is necessary to determine extra spectral values between the original output points either by zero-extending the interferogram and Fourier transforming, or by convolving the original spectral output with a sinc function. Once this is accomplished it is easier to proceed

with the analysis.

The line centers were determined either by using the calculated first and second derivatives of the smooth spectrum or by a technique described in Sec. IV. The uncertainty in the spectral line center was affected by the noise in the data as well as by the blending of neighboring lines. This uncertainty is larger for the lines that are strongly saturated at the line centers, even for the case when these are well isolated from their neighbors. The overall uncertainty in the measured transition frequencies was close to the separation of the spectral points in the interpolated spectrum, i.e., about 0.0004 cm^{-1}.

The absorption contour of a molecular transition in a measured spectrum may be expressed, to a good approximation, by a convolution integral of the true absorption contour and the impulse response (commonly called the instrument function) of the instrument. For the spectrum obtained by using the technique of Fourier spectroscopy, it is more conveniently expressed in the interferogram domain (defined in the optical path difference scale x) rather than in the spectral domain (defined in the wavenumber scale σ). The observed contour $A'(\sigma)$ and the true contour $A(\sigma)$ are related by

$$\int A'(\sigma)\, e^{-i2\pi\sigma x}\, d\sigma = \{\int A(\sigma)\, e^{i2\pi\sigma x}\, d\sigma\}\, T(x), \qquad (1)$$

where $T(x)$ is a multiplicative function of finite extent limited to the maximum optical path difference X in the

interferometer. The function T(x) has a shape which depends on the type of apodization applied to the spectral data. In our case, it is a triangular function tapering to zero at the maximum path difference X;

$$T(x) = 1 - \frac{|x|}{X} \qquad \text{if } |x| \leq X,$$

and

$$= 0 \qquad \text{if } |x| > X. \tag{2}$$

The true absorptance contour of a well-isolated molecular transition line is expressed by

$$A(\sigma) = 1 - \exp\,[-k(\sigma)], \tag{3}$$

where the function $k(\sigma)$ is the absorption coefficient defined by the transition strength S per single molecule in the form

$$\int k(\sigma)\, d\sigma = SN. \tag{4}$$

In this formulation we assume that the absorption is caused by a uniform column of N total molecules per unit cross-sectional area. If thermal equilibrium exists along the absorption path, the strength S is given by the well-known formula

$$S = \frac{8\pi\nu}{3hc} |R|^2 \left(1-e^{\frac{h\nu}{kT}}\right) \frac{1}{g} e^{-E''/kT},$$

where ν is the transition frequency in Hz, R is the transition moment, g is the statistical weight of the lower state, and E" is the lower state energy. The absorption coefficient $k(\sigma)$ takes on various shapes in accordance with the line

profile. If the assumption is valid that collisions from neighboring molecules dominate the spectral line shape, we may express the absorption coefficient by the Lorentzian profile:

$$k(\sigma) = \frac{S\alpha}{\pi[(\sigma-\sigma_o)^2 + \alpha^2]} , \qquad (5)$$

where α is the width and σ_o is the center frequency of the line.

The observed spectrum for most cases contains lines which are to a varying degree overlapped with their neighbors. The absorptance contour for the overlapped lines is given by

$$A(\sigma) = 1 - \exp - [\sum_{n=1}^{N} k_n(\sigma)], \qquad (6)$$

where the absorption consists of N lines, and $k_n(\sigma)$ is the absorption coefficient for the n-th line. The data which we deal with in the analysis contain all possible situations, i.e., from the case of well isolated lines to that of many overlapping lines. The objective of the spectral analysis is to determine the line parameters of each transition, the transition frequency σ_o, and for water the strength S and the width α. We describe below the technique used in extracting these parameters for overlapping lines.

First, we separated the data into groups of lines which were sufficiently isolated and then proceeded to apply a

curve fitting technique based on the least-squares method. The separation of the lines into groups was necessary because the data contained lines of varying degree of overlapping. A criterion was set which established when the absorptance on either side of a line was sufficiently close to zero; the line was then considered to be isolated. With the line center frequency determined as described above, the remaining two variables for each component line (for the case of water), the strength and the width, were determined under the assumption that the line profile was Lorentzian. A spectral pattern theoretically constructed using the Lorentzian profile with assumed parameters was compared with the observed data. The square error between them was calculated and then minimized by adjusting the two variables, the strength and the width, for each component line. The sequence, which was the non-linear least-squares curve fitting process, was repeated to reduce the square error to an expected stationary value according to the noise level in the observed data. Once the error figure converged to a stationary value, the integrated absorptance W, given by

$$W = \int A(\sigma) d\sigma, \tag{7}$$

was calculated for each line contained in the group using the strength and the width thus established. The standard method of obtaining the integrated absorption by numerically integrating the observed absorptance for each line was not

applicable to our data reduction because the data contained considerable overlapping of lines.

III. INSTRUMENTATION

All the measurements were made using the Air Force Geophysics Laboratory (AFGL) high resolution Fourier transform spectrometer with the associated Pfund configuration hot cell. The maximum path difference the interferometer was driven to was 75 cm, resulting in an unapodized resolution of approximately 0.007 cm^{-1}. The AFGL step and hold interferometer (built by Idealab) and hot cell system have been described in previous publications[1,2,3], so will not be described here. However, we would like to indicate one modification in the operation of the system.

In the past, the stepping of the interferometer mirror was controlled with dedicated electronics. With stable external conditions and the gains properly tuned, this hardware stepping system was adequate to step and hold 10^6 steps. However, in practice these conditions were found difficult to achieve and maintain. Consequently, a PDP-8E minicomputer has recently been used to increase the stepping reliability of the interferometer. This mini-computer, used previously only for handling data, is now used to monitor the laser reference signal and take corrective action for the most commonly occurring stepping errors. In addition to relaxing the conditions under which the interferometer can be successfully operated, this computerized stepping control system provides

very useful diagnostic information on the operation of the stepping system. Before the computerized control system was added it was almost impossible to determine anything about the nature of stepping errors that occurred infrequently.

For the actual measurements the high temperature absorption cell, inside the oven, was placed against the entrance window of the interferometer vacuum chamber. Since we were unable to properly couple the hot cell to the interferometer chamber there remained about a 0.25 cm optical path through ambient air. The remainder of the optical path from the source to the interferometer was maintained below 1 torr; except of course when the gases were introduced into the absorption cell when the pressure then was either 3 or 6 torr. The pressure in the absorption cell was measured by a Baratron pressure guage.

IV. CO_2 MOLECULE

The importance of CO_2 as an atmospheric molecule justifies measurements and calculation at high precision of band parameters for a great number of bands; it is indeed a significant contribution to both theoretical and experimental studies of our atmosphere. Very accurate parameters on the (00001-00011)* band of $^{12}C^{16}O_2$ have been obtained by Pine and Guelachvili[4].

---

*For CO_2 there are three fundamental modes of vibration, ν_1, ν_2, and ν_3. Associated with the bending mode, ν_2, is the angular momentum ℓ. The notation used is $v_1v_2\ell v_3r$ where r is the ranking index for a Fermi resonating group.

Their measurement was accomplished by combining two spectra, a room temperature Fourier transform spectrum and a high temperature tunable laser spectrum. There have been numerous measurements of other bands of CO_2, but they were made either with lower resolution spectrometers, near room temperature where fewer rotational lines were excited, resulting in a less accurate determination of band parameters, or electrical discharge spectra where high vibrational levels were obtained but with the normal distribution of rotational level J. In this section we present measurements of CO_2 made with the above described system.

The energy (in cm^{-1}) of a linear molecule, such as CO_2, in a given vibration-rotation state can be represented by

$$E(v,J) = G_v + B_v[J(J+1)] - D_v[J(J+1)]^2 + H_v[J(J+1)]^3$$

where v is the quantum number associated with the vibrational energy, J is the quantum number associated with the total angular momentum of the molecule, and G, B, D are the spectroscopic constants. The infrared spectrum corresponds to transitions between different vibration-rotation states.

The advantages of making the measurements at elevated temperatures are twofold. First, at higher temperatures more rotational lines are excited, making it possible to obtain higher precision in the determination of the spectroscopic constants G, B, D, and H. Secondly, the higher temperature results in higher vibrational energy levels being excited, making more of the so-called "hot bands" measurable.

We used a PDP-8e mini-computer to control the interferometer and to sample the interferogram. The data were taken via magnetic tape to be analyzed at AFGL and/or at the University of Massachusetts. The data were first Fourier transformed, the various lines identified, and finally a least-squares fit technique used to generate new values for the band parameters. Each band was fit independently of the other bands.

Spectra obtained using high resolution Fourier transform spectrometers have an excellent frequency stability over a wide spectral range. There is, however, a small systematic frequency shift introduced into the spectra due to finite detector size. In principle, this correction can be calculated from the geometry of the interferometer apertures and detectors, but in practice it is usually easier to use an internal frequency standard such as lines of CO which were present in our experimental spectra. Guelachvili[5] has measured the positions of these CO lines with an accuracy of 0.00008 cm^{-1}. We used these line positions as an internal frequency standard. After this systematic error was removed from our spectra, the standard deviation of the fit between our data and Guelachvili's, for well isolated lines, was about 0.0004 cm^{-1}.

The identification of the transitions was made in one of three ways, depending on how well the band had previously been measured. For well-known bands the identification

procedure was readily automated. The position and strength of each line was calculated, and then used to locate the line in the experimental spectrum with approximately the right strength that was closest to the calculated position.

For other bands, the positions of lines for low J have been well measured, but not for high J. In this case, the line positions were again calculated and the experimental lines identified, starting at low J and moving up to higher J, until there were not any lines within about 0.02 cm^{-1} of the calculated line. The band was then refit and new constants obtained. The process was iterated until no further extension to higher J was possible.

In some cases the band was so poorly known even at low J that the identification could not be made by taking the experimental line closest to the calculated line position. Another problem arose when certain combinations of merged lines made the extension from low J to higher J impossible. In these two cases, a Loomis-Wood diagram[6] approach has been extremely helpful in picking out the lines that belong to one band in the presence of lines belonging to other bands. When the differences between a calculated line and all observed lines that are nearby are displayed graphically, it is relatively easy to see the pattern created from a set of lines which have spectroscopic constants similar to those used to calculate the line positions.

IV.a. $^{12}C^{16}O_2$ (626)*, 2180 cm^{-1} to 2400 cm^{-1}, 800K

The data presented in this section were obtained at 800K with a resolution of 0.007 cm^{-1}. Once the identification of these measured lines had been made each band was fit discarding only the most severely merged lines. Lines for which the difference between the observed and calculated position was less than about 0.005 cm^{-1} were kept in the fit. All lines used in the fit were weighted equally. The bands that were fit are listed in Table I, along with the standard deviation and the range of J values used. The resulting values obtained for G'-G", B', D', H', B", D" and H" are tabulated in Table II.

Several constraints were used on the fits. The spectroscopic constants H' and H" were constrained to zero for some bands. For bands where ℓ is not equal to zero, ℓ-type doubling results in two sets of energy levels denoted by c and d. The spectroscopic constants obtained for the c and the d levels were considered separately for bands where ℓ=1 and ℓ=2. For the bands where G" is less than 3000 cm^{-1} restrictions were placed on the G's and B's. For ℓ=1 the G's, and for ℓ=2 both the G's and the B's of the c levels were constrained to be equal to those of the d levels.

The difference between the transitions calculated using the band parameters determined by Guelachvili and those in the 1978 AFGL line compilation[8] for the P branch of the

* Designation used on AFGL tapes[7]

Table I. The $^{12}C^{16}O_2$ (626) Bands Observed at 800K

Transition		Band Origin (cm^{-1})	Range of Measurement	Standard Deviation (cm^{-1})
00011	00001	2349.143	P120-R118	0.0009
01111C	01101C	2336.633	P107-R109	0.0007
01111D	01101D	2336.633	P108-R104	0.0006
10012	10002	2327.433	P102-R102	0.0008
02211C	02201C	2324.141	P98-R104	0.0009
02211D	02201D	2324.141	P105-R107	0.0009
10011	10001	2326.598	P104-R104	0.0009
03311	03301	2311.668	P90-R92	0.0009
11111C	11101C	2313.772	P89-R87	0.0009
11111D	11101D	2313.772	P88-R88	0.0012
20013	20003	2305.257	P80-R76	0.0013
12212C	12202C	2302.958	P68-R62	0.0026
12212D	12202D	2302.958	P67-R67	0.0026
04411	04401	2299.214	P82-R83	0.0010
20012	20002	2306.690	P86-R56	0.0013
12211C	12201C	2301.053	P86-R88	0.0010
12211D	12201D	2301.053	P83-R83	0.0010
00021	00011	2324.183	P83-R87	0.0007
20011	20001	2302.523	P82-R78	0.0011
01121C	01111C	2311.703	P90-R80	0.0013
01121D	01111D	2311.700	P83-R79	0.0014
10022	10012	2302.369	P69-R65	0.0018
02221C	02211C	2299.240	P75-R93	0.0013
02221D	02211D	2299.238	P78-R80	0.0012
13311	13301	2288.390	P65-R63	0.0014
13312	13302	2290.680	P73-R66	0.0013

Table II. Spectroscopic Constants for $^{12}C^{16}O_2$ (626) Observed at 800K (cm^{-1})

Band		G"	G' - G"	B'	D'(10^{-7})	H'(10^{-13})	B"	D"(10^{-7})	H"(10^{-1}
00011	00001	0.000	2349.143	.38713745	1.32514	- .1	.39021480	1.32815	- .1
01111C	01101C	667.379	2336.633	.38759128	1.34823	.3	.39063793	1.35387	.2
01111D	01101D	667.379	2336.633	.38818885	1.35624	.2	.39125338	1.35978	.2
10012	10002	1285.409	2327.433	.38750303	1.57182	1.9	.39048172	1.56621	1.8
02211C	02201C	1335.129	2324.141	.38863751	1.37657	- 2.2	.39166830	1.39112	- 2.4
02211D	02201D	1335.129	2324.141	.38863751	1.38347	.8	.39166830	1.38995	.8
10011	10001	1388.187	2326.598	.38706354	1.14847	2.3	.39018922	1.15526	2.3
03311	03301	2003.238	2311.668	.38937836	1.39742	- .4	.39238084	1.41110	- .3
11111C	11101C	2076.865	2313.772	.38735962	1.21874	- 1.2	.39040322	1.23269	- 1.5
11111D	11101D	2076.865	2313.772	.38822645	1.17343	- 2.4	.39132461	1.18134	- 2.4
00021	00011	2349.141	2324.183	.38406499	1.31129	- 2.3	.38714060	1.31706	- 1.9
20013	20003	2548.373	2305.257	.38818763	1.79054	3.8	.39110066	1.79227	3.9
12212C	12202C	2585.032	2302.958	.38894365	1.35669	0.0	.39193107	1.39145	0.0
12212D	12202D	2585.032	2302.958	.38894365	1.48755	0.0	.39193107	1.52141	0.0
20012	20002	2671.146	2306.690	.38652310	1.35362	10.6	.38954825	1.32130	4.6
04411	04401	2671.690	2299.214	.39010454	1.39091	- 1.6	.39307315	1.41071	- 1.7
12211C	12201C	2760.735	2301.053	.38853501	1.34651	-15.0	.39155785	1.39571	-15.0
12211D	12201D	2760.735	2301.053	.38853501	1.32085	6.6	.39155785	1.33752	6.2
20011	20001	2797.154	2302.523	.38747238	.87851	- 4.5	.39057680	.87891	- 4.7
01121C	01111C	3004.016	2311.703	.38456350	1.40044	6.6	.39761095	1.41327	7.3
01121D	01111D	3004.016	2311.700	.38512829	1.34465	- 1.2	.38818842	1.34087	- 2.0
13312	13302	3240.564	2290.680	.38971034	1.47398	0.0	.39265318	1.48599	0.0
13311	13301	3442.256	2288.390	.38924068	1.31704	0.0	.39220963	1.36731	0.0
10022	10012	3612.840	2302.369	.38452333	1.66712	17.0	.38748663	1.58073	3.0
02221C	02211C	3659.277	2299.240	.38560401	1.32035	5.4	.38863983	1.36655	8.4
02221D	02211D	3659.277	2299.238	.38556943	1.28275	- 6.1	.38859689	1.28382	- 6.4

02201C - 02211C band of $^{12}C^{16}O_2$ is shown in Figure 1. Guelachvili made extremely accurate room temperature measurements (0.0001 cm^{-1}) of the positions of transitions up to about J = 46 of this band, from which he calculated spectroscopic constants[9]. For J < 50 the agreement with our data is excellent, but for high J the difference is large.

The large values of the standard deviations given in Table I, considerably greater than the 0.0004 cm^{-1} for well isolated lines mentioned earlier, are caused by merging from overlapping bands. Most observed lines are merged to some degree. If the overlapping lines belong to bands that are not correlated with the band being fit, the effect of the merged lines will be to produce an increase in the random scatter of the fit. It is very rare to have both the position and the spacing between the lines of the band being fit and the lines in a merging band close enough that significant correlation occurs. The strongest correlation between bands in the observed spectrum appears to be between c and d bands. For example, the 01101C-01111C and the 01101D-01111D bands have spectroscopic constants just different enough that even though they have the same band origin, R(105) of the c band is merged with R(106) of the d band. At this point in the bands, the difference between the line spacing is only 0.005 cm^{-1}, yet R(103) is not merged with R(104), nor is R(107) merged with R(108). The smallness of the correlation between

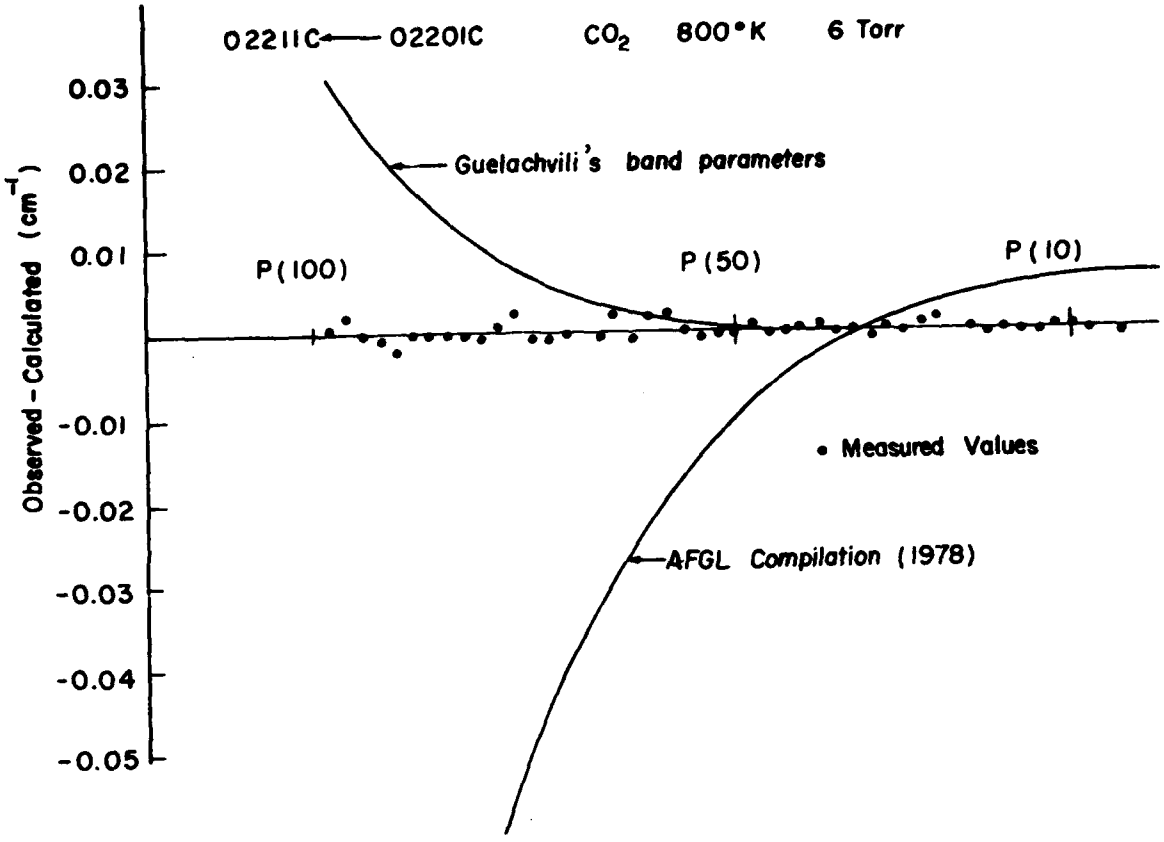

Figure 1. Comparison of the line positions for the P branch of the (02211C-02201C) band between our values measured at 800K and those extrapolated from other room temperature data. Guelachvili's measurement at room temperature extends up to P46 lines, while the 1978 AFGL compilation is based on the old data.

bands supports the assumption that fitting partly merged lines does not introduce systematic errors.

To further insure that the identification and fitting procedure was valid, a synthetic spectrum was calculated and compared to the observed spectrum. The spectroscopic constants listed in Table II and the band intensities given in reference 7 were used to create the synthetic spectrum. Bands that resulted in higher absorption in the synthetic than in the observed spectrum were either refit or thrown out entirely.

IV.b. $^{13}C^{16}O_2$ and $^{13}C^{16}O^{18}O$; 2140 cm^{-1} to 2340 cm^{-1}, 600K

Spectroscopic constants for $^{13}C^{16}O_2$ and $^{13}C^{16}O^{18}O$ that predict the position of spectral lines for J values greater than 100 were obtained from absorption data of an isotopically enriched sample of CO_2. The gas sample, consisting of 88% $^{13}C^{16}O_2$, 11% $^{13}C^{16}O^{18}O$ and 1% various other isotopes, was heated to a temperature of 600K. By making measurements on several isotopes a more accurate determination of the electric potential for the CO_2 molecule can be made since the electric potential function is identical for different isotopes of the same molecule.

Each spectrum was computed by averaging three transformed interferograms, each of which had a measurement time of fifteen hours. Spectra were taken at both 300K and 600K, but only results of analysis of the 600K spectrum containing high J lines are presented. The 300K spectrum was taken in order to assist in the identification of $^{13}C^{16}O^{18}O$ bands in

the 600K spectrum.

To eliminate the effects of a sloping background, a spectrum was taken of the empty absorption cell and the desired spectrum was ratioed against this spectrum. To minimize the effects of noise in the empty-cell spectrum a 13 point running average was first used to smooth the spectrum before the ratioing was performed.

The spectrum was then analyzed to obtain the position, asymmetry, width, and strength of each line. The density of the spectral points was increased by a factor of sixteen through interpolation. The line positions were determined by taking the wave number position of the point closest to the local minimum as the line center location. A measure of line asymmetry was given by using an alternative method for finding the line positions and comparing the results of the two methods. This second method used the center of a chord drawn across the absorption line a small distance up from the minimum to determine the line center. For symmetric lines, the center of this chord coincides with the line position found from the local minimum method. The line width was determined as being proportional to the length of this chord. An estimate of line strength was calculated by integrating the area between the spectral line and the background. The asymmetry, width, and line strength were used to determine the amount of line merging present and hence the quality of each line.

As a check on the quality of the experimental data a comparison of the line positions of the 00001 to 00011 band of $^{12}C^{16}O_2$, observed from P(72) to R(78) was made with the line positions computed using the spectroscopic constants given by Pine and Guelachvili[4]. The results of this comparison showed a systematic difference of 0.0001 cm^{-1} and an rms error of 0.0008 cm^{-1}.

For low J lines, identification was accomplished by assigning the line in the experimental spectrum whose position was closest to the position calculated using the AFGL (1980) spectroscopic constants[11]. The lines were identified starting from low J and moving up to higher J until there weren't any lines close (within about 0.02 cm^{-1}) to the calculated values. The band was then refit, new constants obtained, and the process iterated until further extension to higher J was impossible. For the ν_3 fundamental band of $^{13}C^{16}O^{18}O$ it was not possible to make conclusive identification of the lines in the 600K spectrum, without first using the AFGL (1980) constants to identify the lines in the 300K spectrum. The band was first fit using the 300K data. The resulting constants were then used to make the identification in the 600K spectrum.

After the lines were identified, a fit was then performed on each band. All lines within 0.0025 cm^{-1} of the calculated positions were kept in the fit. In order to insure that the identification process was working properly, lines that were

not included in the fit were checked for asymmetry and abnormally large width or strength to verify that their exclusion from the fit was justified. All lines used in the fit were weighted equally. The bands that were fit are given in Table III along with the range of J values, the total number of lines, and the standard deviation of each fit. The resulting values obtained for G'-G", B', D', B", and D" are tabulated in Table IV. All spectroscopic constants were allowed to float freely in the fit. No attempt was made to combine these constants in such a manner as to yield a single consistent potential function for the CO_2 molecule.

For the 00001 to 00011 and the 01101 to 01111 bands of $^{13}C^{16}O_2$ the low J lines were badly saturated. Guelachvili had previously measured these lines to a high accuracy[9], hence for low values of J the line positions of Guelachvili were used in the fit. Guelachvili's line positions were used for the P(52) to R(50) lines of the 00001 - 00011 band, from P(35) to R(25) for the 01101C - 01111C band, and from P(40) to R(40) for the 01101D-01111D band.

Comparisons of the line position measurements determined in this work to those predicted by the extrapolation using Guelachvili's constants[9] and those used in the 1980 AFGL line compilation[11] are given in Figures 2 to 4.

Several interesting features are illustrated by these figures. Although Guelachvili's line positions were measured with considerably more accuracy than ours, extrapolation to

Table III. Isotopic CO_2 Bands Observed at 600K

Transition	Isotope	Band Origin cm^{-1}	Range of Measurement	Number of Lines Used	Standard Deviation (cm^{-1})
00011 00001	636	2283.4876	P(114) - R(116)	101	0.0008
01111C 01101C	636	2271.7604	P(109) - R(107)	91	0.0009
01111D 01101D	636	2271.7603	P(110) - R(110)	101	0.0008
10012 10002	636	2261.9098	P(98) - R(100)	87	0.0012
02211C 02201C	636	2260.0500	P(100) - R(100)	67	0.0012
02211D 02201D	636	2260.0498	P(97) - R(99)	66	0.0010
10011 10001	636	2262.8487	P(98) - R(98)	69	0.0011
00011 00001	638	2265.9730	P(97) - R(100)	144	0.0010

Table IV. Spectroscopic Constants for Isotopic CO_2 Observed at 600K (cm^{-1})

Transition		Isotope	G'-G"	B'	D'(10^{-7})	B"	D"(10^{-7})
00011	00001	636	2283.4876	0.38727477	1.32699	0.39023879	1.33112
01111C	01101C	636	2271.7604	0.38767386	1.33881	0.39060523	1.34555
01111D	01101D	636	2271.7603	0.38829031	1.35288	0.39124131	1.35669
10012	10002	636	2261.9098	0.38802165	1.53779	0.39090059	1.54245
02211C	02201C	636	2260.0500	0.38871619	1.35576	0.39163183	1.36918
02211D	02201D	636	2260.0498	0.38868963	1.36587	0.39160487	1.37338
10011	10001	636	2262.8487	0.38670201	1.15853	0.38969557	1.16111
00011	00001	638	2265.9730	0.36538830	1.18047	0.36817867	1.18394

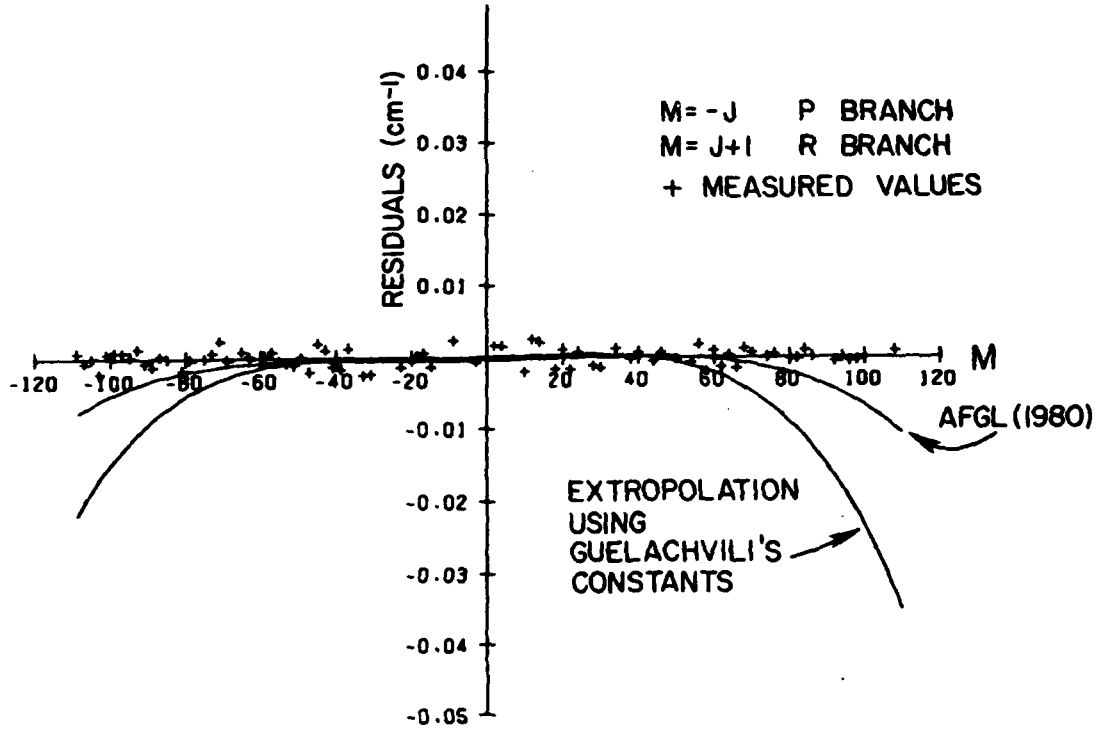

Figure 2. Comparison of measured line positions with those computed using Guelachvili's and the AFGL (1980) constants for the 01101C to 01111C band of $^{13}C^{16}O_2$.

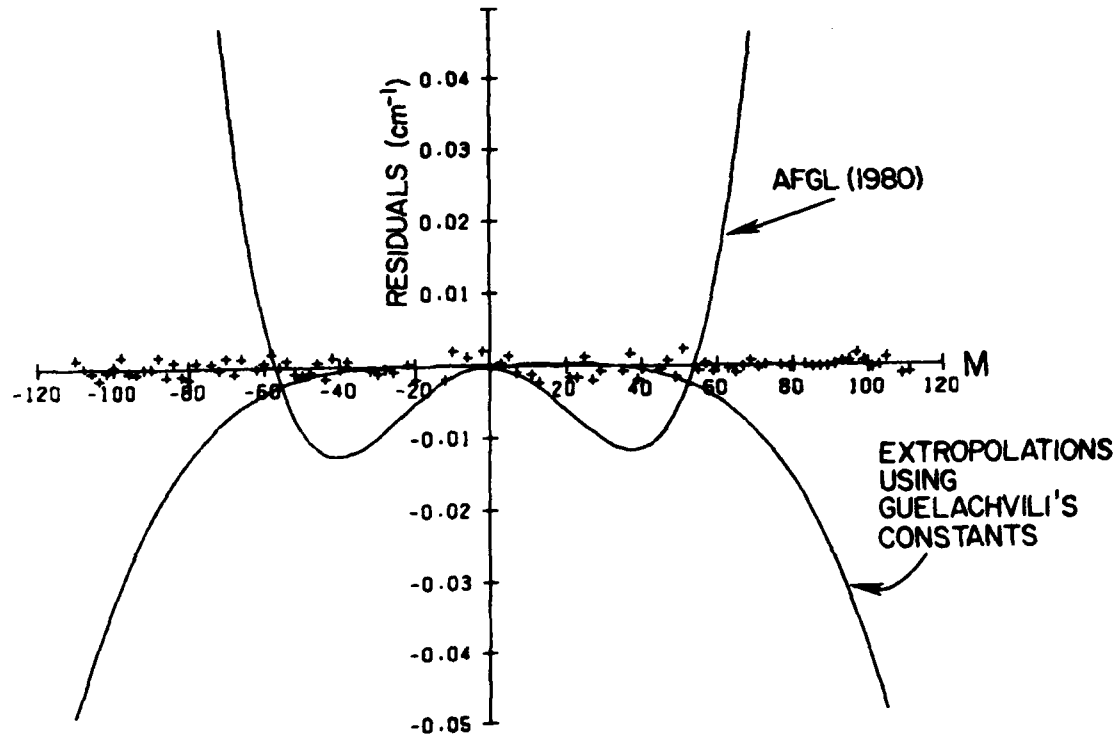

Figure 3. Comparison of measured line positions with those computed using Guelachvili's and the AFGL (1980) constants for the 01101D to 01111D band of $^{13}C^{16}O_2$.

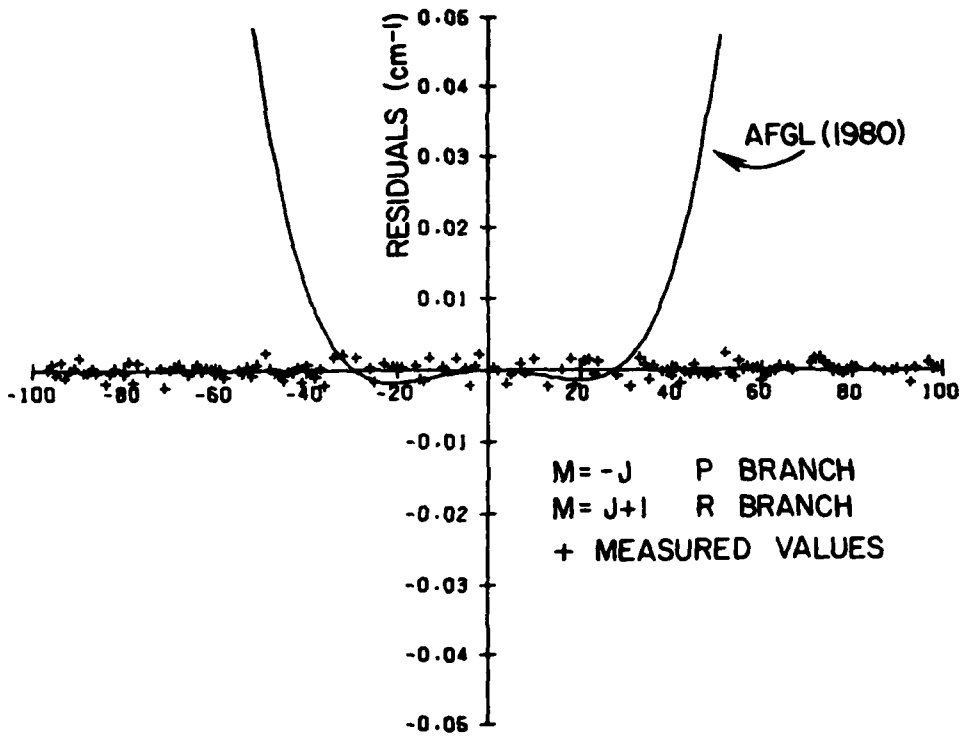

Figure 4. Comparison of measured line positions with those computed using the AFGL (1980) constants for the 00001 to 00011 band of $^{13}C^{16}O^{18}O$.

higher J (higher temperature) is unsatisfactory. It appears to be a general principle that spectroscopic constants obtained using low J lines do not successfully predict the position of high J lines. By comparing the difference in the quality of the AFGL (1980) fit of the 01101C-01111C band to the D band it can be seen that the AFGL (1980) line compilation is quite good for some of these very weak atmospheric bands while not for others. The spectroscopic constants for the eight bands reported in this section predict the position of spectral lines to an estimated absolute accuracy of 0.001 cm^{-1} for J values up to 100. This represents a significant improvement in the accuracy with which high J line positions of the isotopes $^{13}C^{16}O_2$ and $^{13}C^{16}O^{18}O$ can be computed. This improvement illustrates the advantage of heating the sample to determine spectroscopic constants that are valid for large J values. For several of these bands a positional accuracy improvement was realized for low J lines as well.

IV.c. $^{13}C^{16}O_2$ and $^{13}C^{16}O^{18}O$; 2140 cm^{-1} to 2340 cm^{-1}, 800K

In this section we present results of measurements of the same isotopic species as the previous section but at a temperature of 800K.

A total of four 800K spectra were taken, two with a CO_2 gas pressure of 3 torr and two with 6 torr. In addition to these four spectra, several empty hot cell spectra were also recorded to be used as a reference. The measurement time for each spectrum was approximately fifteen hours.

After the two 3 torr spectra and the two 6 torr spectra were each separately co-added they were ratioed by the empty cell reference spectrum to reduce background effects. To minimize noise in the empty cell spectrum a thirteen point running average was first used to smooth the spectrum before the ratioing was performed. The 3 torr and the 6 torr spectra were then analyzed as described in Sec. IV.b. to obtain the position, asymmetry, width, and strength of each line.

The asymmetry, width, and line strength were used to determine the amount of line merging present and hence the quality of each line. Only severely merged lines were excluded from the least squares procedure. Lines which were slightly merged were still used but with a reduced weighting. The weight associated with each line, the reciprocal of the expected uncertainty squared, was estimated from the line asymmetry, abnormal line width, and inconsistencies of line position as computed from other lines in the band. Before the final fit was realized the 3 torr and 6 torr data were combined to form a single set of data.

Since there was a small amount of $^{12}C^{16}O_2$ in the high temperature cell it was possible to make a check on the quality of the experimental data by comparing the line positions observed from P(66) to R(84) of the 00001 to 00011 band with the line positions computed using the spectroscopic constants given by Pine and Guelachvili[4]. The results of this comparison showed evidence for the existence of a systematic error,

particularly for the weak lines at the high end of the R branch where the systematic difference reached a maximum of 0.0006 cm^{-1}. This error probably resulted from incomplete phase correction. The average difference was less than 10^{-4} cm^{-1} with a rms difference of 0.0003 cm^{-1}.

A weighted least squares fit was then performed on each band. An example of the quality of the fit and the data used is given in Table V for the P branch of $^{13}C^{16}O_2$ for the 00001 to 00011 band. This table lists the observed line position, line identification, difference between observed and calculated position, and the expected uncertainty for each line.

Since the low J lines for the 00001 to 00011 band of $^{13}C^{16}O_2$ were badly saturated for both the 3 torr and 6 torr spectra, lines from P(40) to R(40) of this band were excluded from the fit.

The bands that were fit are given in Table VI, along with the range of J values, the total number of lines used, and the standard deviation of each fit. The resulting values obtained for G'-G", B', D', H', B", D", and H" are tabulated in Table VII. All spectroscopic constants were first allowed to float freely in the fit. The resulting values of H' and H" were smaller than the uncertainty in these parameters for some bands, therefore H' and H" were constrained to zero. These bands are designated in Table VII by letting H' = H" ≡ 0.

Table V. The P-Branch of the 00001 to 00011 Band of $^{13}C^{16}O_2$ (636)

Assignment	Observed	Observed Minus Calculated	Expected Uncertainty
P(42)	2245.6445	0.0001	0.0010
P(44)	2243.5859	0.0002	0.0008
P(46)	2241.5038	-0.0001	0.0008
P(48)	2239.4004	0.0013	0.0017
P(50)	2237.2715	0.0004	0.0005
P(52)	2235.1204	0.0002	0.0009
P(54)	2232.9463	0.0001	0.0005
P(56)	2230.7495	0.0002	0.0005
P(58)	2228.5298	0.0004	0.0005
P(60)	2226.2873	0.0006	0.0008
P(62)	2224.0212	0.0002	0.0004
P(64)	2221.7328	0.0003	0.0005
P(66)	2219.4215	0.0003	0.0004
P(68)	2217.0873	0.0001	0.0004
P(70)	2214.7288	-0.0015	0.0013
P(72)	2212.3504	-0.0004	0.0005
P(74)	2209.9480	-0.0005	0.0007
P(76)	2207.5236	-0.0000	0.0004
P(78)	2205.0754	-0.0007	0.0005
P(80)	2202.6041	-0.0018	0.0012
P(82)	2200.1125	-0.0007	0.0005
P(84)	2197.5983	0.0003	0.0007
P(86)	2195.0597	-0.0006	0.0005
P(88)	2192.5003	0.0002	0.0006
P(90)	2189.9165	-0.0009	0.0011
P(92)	2187.3105	-0.0019	0.0012
P(94)	2184.6860	0.0010	0.0010
P(96)	2182.0354	0.0002	0.0004
P(98)	2179.3648	0.0016	0.0013
P(100)	2176.6696	0.0007	0.0007
P(102)	2173.9520	-0.0003	0.0004
P(104)	2171.2127	-0.0008	0.0011
P(106)	2168.4526	0.0000	0.0003
P(108)	2165.6698	0.0003	0.0004
P(112)	2160.0387	0.0016	0.0013
P(114)	2157.1878	-0.0000	0.0006
P(116)	2154.3160	-0.0006	0.0011
P(118)	2151.4217	-0.0016	0.0023
P(120)	2148.5085	0.0003	0.0011
P(122)	2145.5735	0.0024	0.0024

Table VI. Isotopic CO_2 Bands Observed at 800K (cm^{-1})

Transition	Isotope	Band Origin (cm^{-1})	Range of Measurement	Number of Lines Used	Standard Deviation ($10^{-4} cm^{-1}$)
00011 00001	636	2283.4877	P(122)-R(122)	80	4
01111C 01101C	636	2271.7605	P(113)-R(107)	101	4
01111D 01101D	636	2271.7602	P(116)-R(112)	105	3
10012 10002	636	2261.9102	P(104)-R(104)	96	4
02211C 02201C	636	2260.0500	P(106)-R(104)	88	4
02211D 02201D	636	2260.0501	P(103)-R(103)	84	4
10011 10001	636	2262.8486	P(104)-R(98)	89	5
00011 00001	638	2265.9719	P(102)-R(100)	176	4

Table VII. Spectroscopic Constants for Isotopic CO_2 Observed at 800K (cm^{-1})

Transition	Isotope	G'-G''	B'	D'(10^{-7})	H'(10^{-13})	B''	D''(10^{-7})	H''(10^{-13})
00011 00001	636	2283.4877	0.38727068	1.32514	0	0.39023480	1.32934	0
01111C 01101C	636	2271.7605	0.38767635	1.34213	0	0.39060780	1.34897	0
01111D 01101D	636	2271.7602	0.38828848	1.35159	0	0.39123954	1.35550	0
10012 10002	636	2261.9102	0.38802951	1.55698	1.133	0.39090892	1.56254	1.175
02211C 02201C	636	2260.0500	0.38869109	1.29446	-3.856	0.39160593	1.30477	-4.129
02211D 02201D	636	2260.0501	0.38868939	1.36350	-0.300	0.39160473	1.37074	-0.336
10011 10001	636	2262.8486	0.38672090	1.19442	2.142	0.38971481	1.19792	2.190
00011 00001	638	2265.9719	0.36538985	1.18096	0	0.36817985	1.18410	0

For the bands where ℓ-type doubling is present the c and d levels were fit independently. Since the band origins resulting from fitting the c levels should be identical to the one resulting from the d levels, a check on the precision of the data can be obtained by comparing the difference between the two. The difference between the band origins for the 01101 to 01111 transitions was 0.0003 cm^{-1}, and for the 02201 to 02211 transitions was 0.0001 cm^{-1}.

Comparisons of the line position measurements determined in this work to those predicted by the constants used in the 1980 AFGL line compilation and Guelachvili's constants for those bands which he measured[9] are given in Figs. 5 through 12. Several interesting features are illustrated by these figures. Although Guelachvili's line positions were measured with considerably more accuracy than ours, extrapolation to higher J (higher temperature) was unsatisfactory, as shown in Figs. 5 through 7. However, interpolating from high J to low J seems to work quite well as indicated by the comparison shown in Fig. 5 between the fit of the 00001 - 00011 band of $^{13}C^{16}O_2$, excluding lines from P(40) to R(40), and the measurements of Guelachvili. The difference in the band center as compared to Guelachvili's for this band was only 0.0002 cm^{-1}. Table VIII is a listing of the lines used in the fit.

By comparing the difference in the quality of the AFGL (1980) fit of the 01101C-01111C band to the D band (Figs. 6

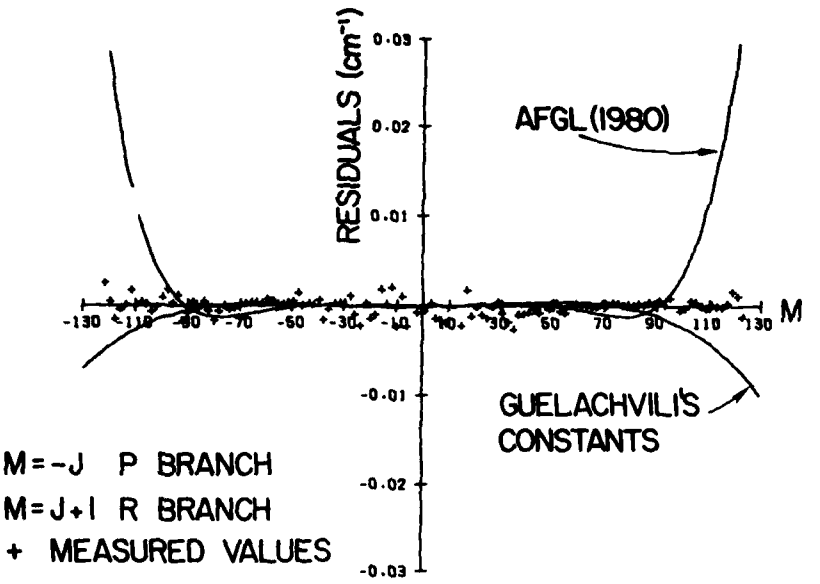

Figure 5. Comparison of measured line positions with those computed using Guelachvili's and the AFGL (1980) constants for the 00001 to 00011 band of $^{13}C^{16}O_2$.

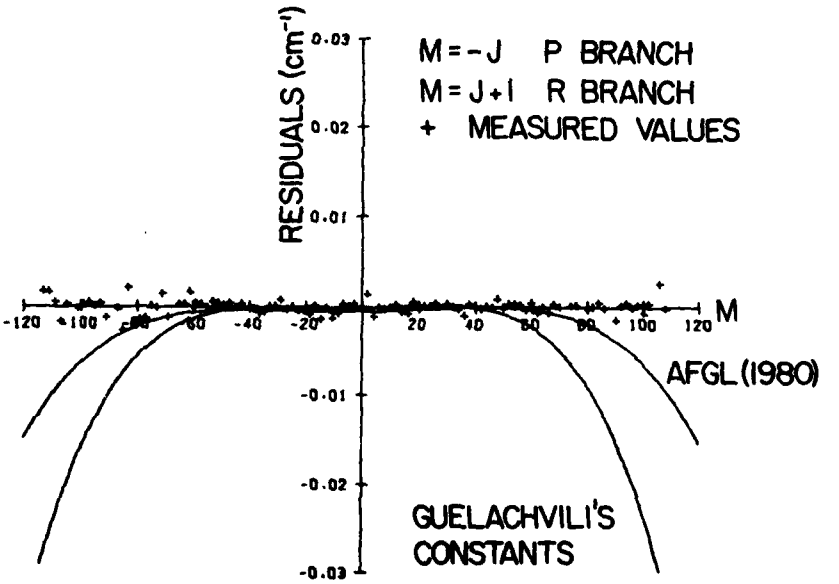

Figure 6. Comparison for the 01101C to 01111C band of $^{13}C^{16}O_2$.

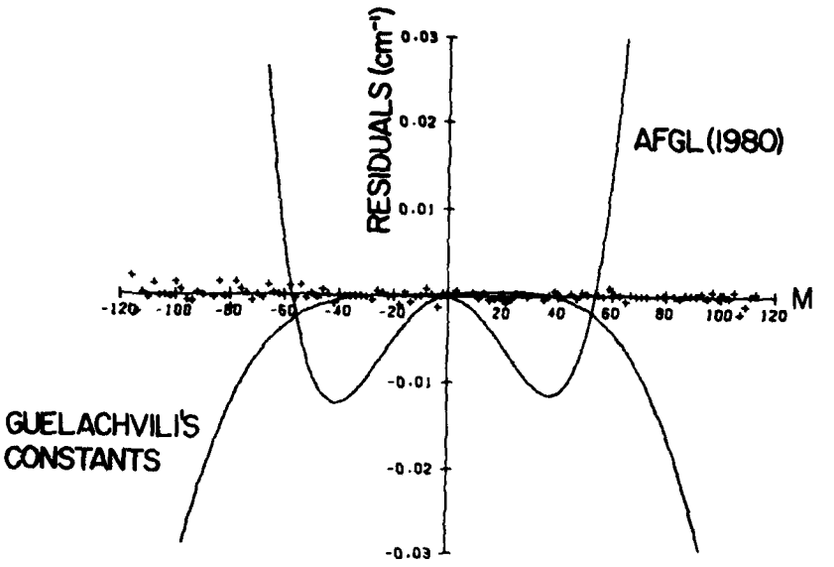

Figure 7. Comparison for the 01101D to 01111D band of $^{13}C^{16}O_2$.

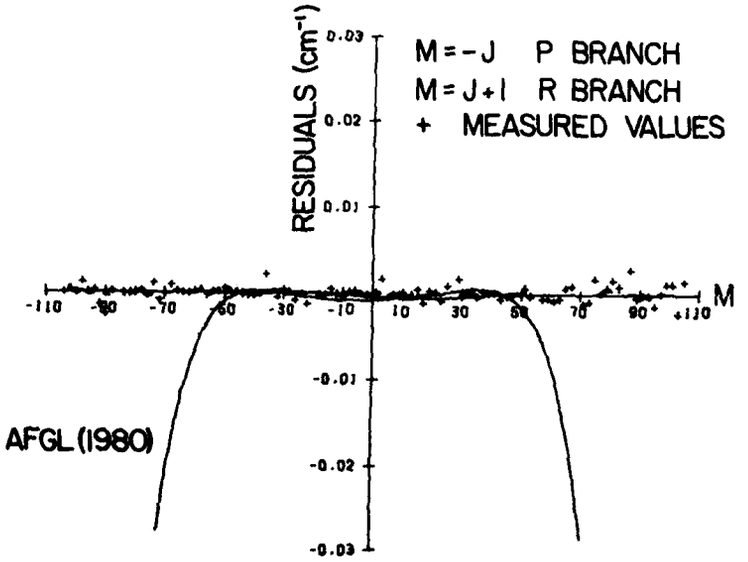

Figure 8. Comparison for the 10002 to 10012 band of $^{13}C^{16}O_2$.

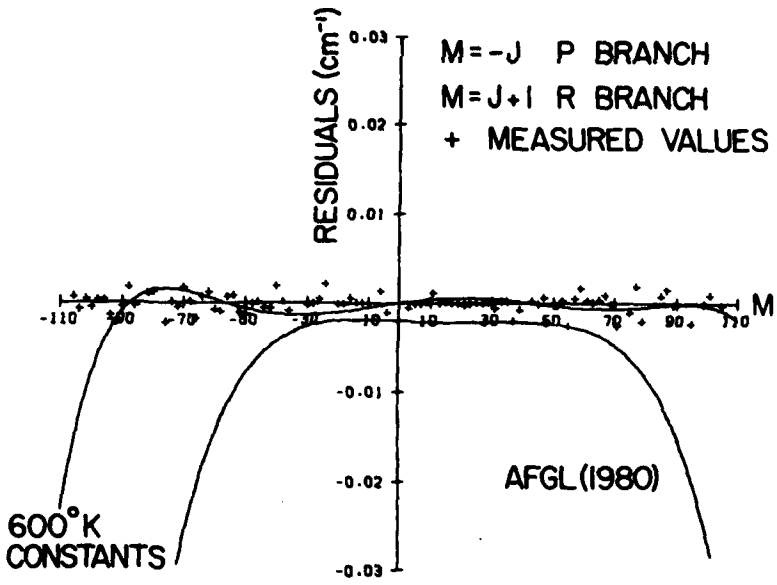

Figure 9. Comparison for the 02201C to 02211C band of $^{13}C^{16}O_2$.

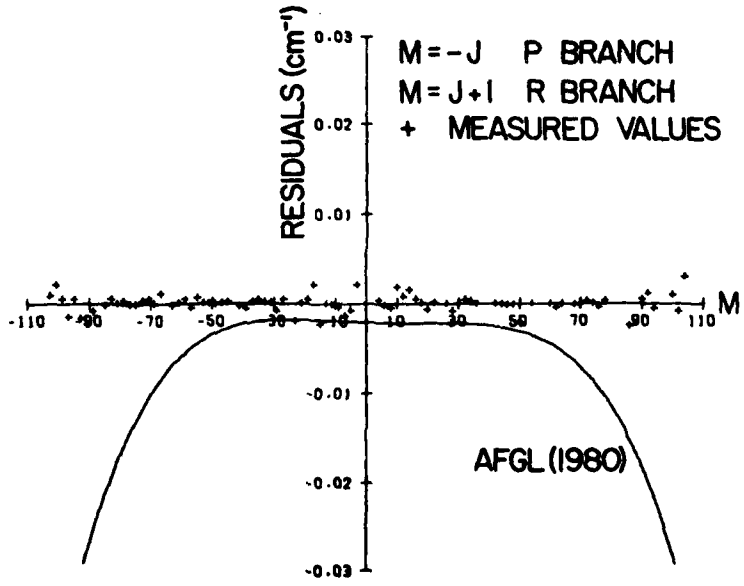

Figure 10. Comparison for the 02201D to 02211D band of $^{13}C^{16}O_2$.

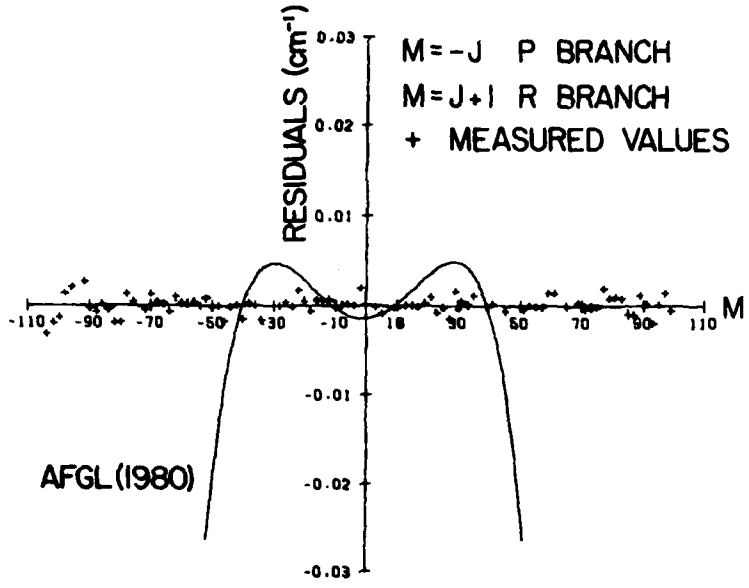

Figure 11. Comparison for the 10001 to 10011 band of $^{13}C^{16}O_2$.

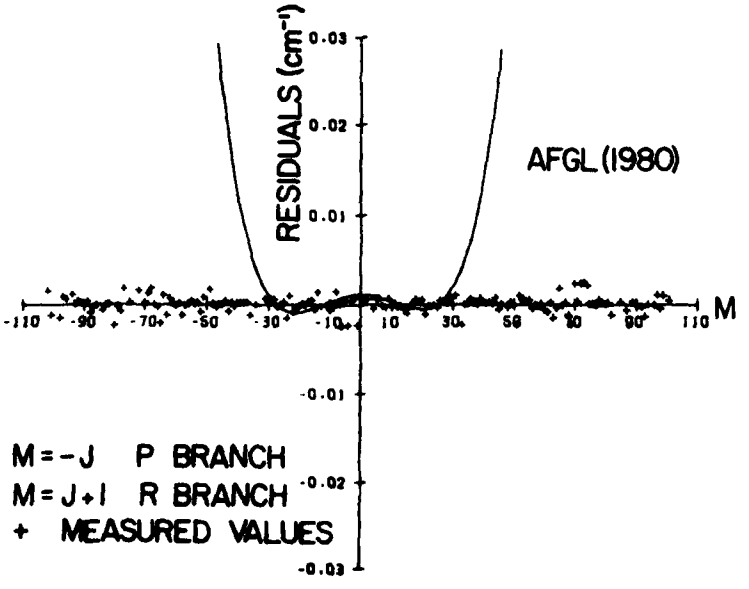

Figure 12. Comparison for the 00001 to 00011 band of $^{13}C^{16}O^{18}O$.

and 7) it can be seen that the constants used for the AFGL (1980) line compilation are quite good for some of these very weak atmospheric bands but not so good for others.

The improvement in the spectroscopic constants obtained at 800 K over those of the previous section for 600 K are not particularly significant except for the 02201C to 02211C band of $^{13}C^{16}O_2$ where the P branch shows a marked difference (Fig. 9). Using the expansion in powers of J(J+1) (Eq. 1) to extrapolate from a lower to a higher J is unsatisfactory, particularly for this band as indicated by the poor positional accuracy of high J lines predicted using both the AFGL (1980) constants and the 600 K constants. Also, there is a tendency for oscillations in the fit. The H values obtained for this band are unusually large and negative. Large negative H's were also reported[12] (table II of Sec. IV.a.) for these same two vibrational levels 02201C and 02211C for the main isotope $^{12}C^{16}O_2$.

The spectroscopic constants for the eight bands reported in this section predict the position of spectral lines to an estimated absolute accuracy of better than 0.001 cm^{-1} including J values greater than 100. This represents a significant improvement in the accuracy with which high J line positions of the isotopes $^{13}C^{16}O_2$ and $^{13}C^{16}O^{18}O$ can be computed.

V. H_2O (161); 1600 cm^{-1} to 2001 cm^{-1}, 800K

In this section we present results of measurements of H_2O using the instrumentation and the analysis technique

described above.

A Lorentzian profile was assumed as the line shape in our analysis — which is probably improper in principle. However, the H_2O data were always taken at very low pressure in order to reduce to a minimum the line overlapping problem. The expected collision width was much smaller than the Doppler width under such a condition. The Lorentz line shape was adopted because of the following reasons. For weak lines the question of line width is irrelevant because the integrated absorptance W and the strength maintain a linear relationship independent of width. For strongly saturated lines, the observable absorptance contour corresponded to the wing region of the line which was Lorentzian. The central peak region of such lines was completely saturated. The integrated absorption W was controlled by the wing section and thus by the Lorentzian profile. The line profile in the center peak region produced only a small effect in the determination of the integrated absorptance. Thus the Lorentzian profile assumption was a proper practical choice for obtaining the integrated absorptance even though it was theoretically improper.

Once the integrated absorptance was determined, it was used to derive a value for the final strength. For the Lorentzian line which was strongly saturated at the center, the strong interdependence existing between the strength S and the width α made their separate determination very

impractical. With the integrated absorptance and the absorptance contour fixed, a quantity $\sqrt{S\alpha}$ was the only meaningful parameter which could be determined for such a line, even when the noise level in the data was exceptionally small. We adopted the theoretically accepted value for α (Ref. 13) in deriving the strength from the integrated absorptance. The width was extrapolated at 800K from the values calculated for room temperature using a simple impact theory assumption;

$$\alpha\ (T) = \alpha\ (T_o)\ \left(\frac{T_o}{T}\right)^{1/2} .$$

The results obtained for water vapor are summarized in Table IX. The data listed in the table are the line frequency in cm^{-1}, the intensity S in (cm^{-1}/molecule cm^{-2}) at 800K, the observed integrated absorptance for an observation condition P_{H_2O} = 6.0 torr, T = 800K and ℓ = 350 cm, the lower state energy in cm^{-1}, the transition identification (J', Ka', Kc'), (J", Ka", Kc"), (v'_1, v'_2, v'_3) and ($v"_1$, $v"_2$, $v"_3$), and the difference between the observed transition frequency and the value listed in the latest AFGL line listing[11]. The data are arranged in ascending order of observed line position. The data listed in Table IX contain those lines newly identified in the present study, which are the high J lines of the (ν_2-O) and the ($2\nu_2$-ν_2) transitions. We were able to follow the ν_2 transitions up to the $(24_{1,24}-23_{0,23})$-$(24_{0,24}-23_{1,23})$ doublet, and the ($2\nu_2$-ν_2) transition up to the $(20_{1,20}-19_{0,19})$-$(20_{0,20}-19_{1,19})$ doublet. The highest

excitation energy observed at 800K in our data exceeded 5000 cm^{-1}. Table X summarizes those lines which were either newly assigned or quite different from the latest AFGL line listing.

VI. Global Constants for Carbon Dioxide.

One of the principal aims of the research described in this report has been to provide data from which reliable parameters, necessary for high resolution atmospheric transmission/emission calculations, could be obtained. In this section we describe the application of the AFGL FTS-hot cell measurements on CO_2 to the determination of "global constants". This approach is to be distinguished from the discussion in Sec. IV, where vibration-rotation bands were least-squares fit independently to obtain spectroscopic constants that would best reproduce that particular band with the minimum root-mean-square deviation, regardless of the fact that the vibrational levels involved in the transition are themselves part of an ensemble of many vibrational levels connected by allowable electric dipole transitions. In the approach for global constants, all connected vibrational states that have been observed at high resolution (in the laboratory) are taken in concert. The approach is analogous to forming a "tree" and bootstrapping to successive vibrational levels. For each isotopic species we thus require the constants to form a self-consistent set. In general the deviations between observed and calculated positions of transitions will now be

slightly larger than the best fit of individual bands, depending on the weakest link in the path, either the accuracy of the measurement of a band, or more usually, the limit of the highest value of rotational quantum number observed. Nevertheless, a great consistency has been realized by this method for generating the line positions of the approximately 560 vibration-rotation bands of importance to atmospheric optics problems in the IR, covering a spectral range of 400 to 10,000 cm^{-1}. The method has been discussed somewhat in Ref. 10, but several points will be elaborated upon here. It should be remarked that this method does not go to the extent of combining the various isotopic measurements completely to form a true valence bond force potential, (see for example ref. 14) but treats them quasi-independently, only making extrapolations for the other isotopes where measurements have not been made. Common to both approaches, as has been discussed in Sec. IV, is the difficulty in making accurate predictions of rotational levels much beyond the highest measurements. It is indeed this aspect that has made the results of the measurements of the high temperature CO_2 at AFGL such a step forward in the determination of good parameters since the calculation of intermediate rotational levels is reliable and hence the extension of J-values that has been described here has greatly extended the reliability of line parameter compilations.

We first review some of the considerations involved in

a description of the energy level and rotational constants for CO_2. For a linear triatomic molecule like CO_2, the vibrational states are characterized by three quantum numbers, which are zero or positive integers, of pure vibration, v_1, v_2, and v_3 and a fourth number $\ell = v_2, v_2-2, \ldots -v_2 + 2, -v_2$ which represents the contribution of the bending mode to angular rotation. In order to calculate the purely vibrational part of the energy, it is necessary first to compute an unperturbed energy,

$$G_v^{unp} = \sum_i \omega_i v_i + \sum_{ij} x_{ij} v_i v_j + g_{22}\, \ell^2 + \sum_{ijk} y_{ijk} v_i v_j v_k + \sum_i y_{i\ell\ell}\, v_i\, \ell^2 + \ldots \tag{8}$$

and then to incorporate the effects of resonance perturbation by combining all close-lying levels with common ℓ and common symmetry in matrices whose diagonal elements are G_v^{unp}, whose off-diagonal elements are functions of additional molecular constants and the four quantum numbers, and whose eigenvalues are the vibrational energy G_v.

This perturbation calculation results in the "mixing" of states whose G_v^{unp} are particularly close, so that the final description of the level by the original four quantum numbers is a poor one. Accordingly, it is useful to add a fifth index, the rank symbol r to label all such mixed states in order of decreasing energy. We have adopted this procedure for CO_2, where the mixed states are $(v_1\ v_2\ \ell_2\ v_3)$, $(v_1 + 1,$

$v_2 - 2, \ell_2, v_3)$, . . . etc. The highest value of v_1 and the lowest value of v_2 in each set are retained in the vibrational identification for all levels of the set.

There is an accidental (Fermi) resonance between the vibrational states v_1 and $v_2 = 2v_1$. The wave functions become a mixture of each of the two states contributing to each perturbed level.

We describe the energy levels by $v_1 v_2 \ell v_3 r$, where the ranking index, r, is unity for the highest vibrational level of a Fermi resonating group. The ranking index can assume the values 1, 2, .. $v_1 + 1$. The quantum numbers v_2 and ℓ are always equal in the AFGL notation.

It will be noted in Eq. (8) that the vibrational energy depends on ℓ^2. When $\ell \neq 0$ there are two levels for each $J \geq \ell$, and this degeneracy is removed by rotation. The splitting ("ℓ-type doubling") results in two sets of levels, designated c and d, with different effective rotational constants. When $\ell = 1$ the splitting is most important, and $B_c \neq B_d$, $D_c \neq D_d$, etc.; when $\ell = 2$, $B_c = B_d$ but $D_c \neq D_d$, etc.; when $\ell = 3$, the constants other than H are the same. These results are rigorous and arise from the effect of removing the degeneracies. For the pi-states ($\ell = 1$) one performs a single contact transformation and the off-diagonal terms have the effect of a term in J(J+1), i.e., change the effective B-rotational constant. For delta-states ($\ell = 2$), the coupling between diagonal numbers is twice removed, necessitating a

double contact transformation which has the effect of $J^2(J+1)^2$. This first affects the fourth order or D-centrifugal stretching constant. Resonances occasionally cause larger deviations, such as might be seen in some of the H_v constants.

When the linear molecule has a center of symmetry, as in CO_2 with ^{16}O at both ends (but not when one oxygen is isotopically different), the paired atoms with zero nuclear spin cause zero statistical weight for rotational levels of a given parity. Thus, only even-J levels exist for the ground vibrational level and for all other levels with $\ell = 0$ and v_3 even ("Σ_g^+ symmetry"); for levels with $\ell = 0$ and v_3 odd (Σ_u^-), only J odd exists; when $\ell > 0$, the c- and d- sublevels have different symmetry, so that for $\ell = 1$, $v_3 = 0$ (Π_u) the J = odd levels are c and the J = even levels are d, etc. In the AFGL compilation, symbols c or d are appended to the rotational quantum number of the lower state only when required, that is for $\ell \geq 1$ in the molecules without the center of symmetry. For example, R27C means 28c ← 27c; Q27C means 27d ← 27c. Figure 13 illustrates this scheme for point group $C_{\infty v}$ for the first few lines of a Π-Π transition.*

The line frequencies are determined from the energy states by taking the differences corresponding to all allowed transitions. These depend on the familiar selection rules

*It should be noted that the c and d labels correspond respectively to the new standardized e and f labelling of parity doublet levels (see Ref. 15).

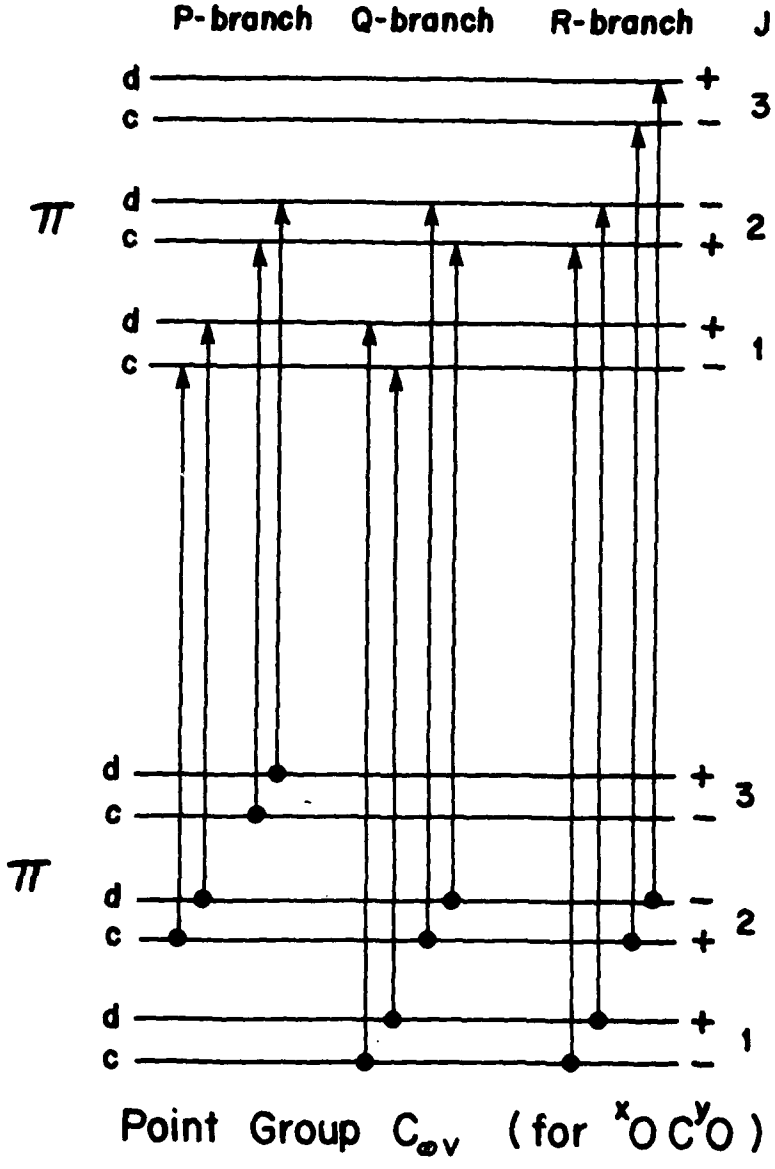

Figure 13. Designation of c- and d- levels for Π-Π transition for CO_2 without center of symmetry.

for the linear molecule:

when $\Delta \ell = 0, \Delta J = \pm 1$, c ↔ c, d ↔ d,

when $\Delta \ell = 1, \Delta J = \pm 1$, c ↔ c, d ↔ d,

and also $\Delta J = 0$, c ↔ d.

The line positions may thus be conveniently represented for computational purposes as a given series in $\underline{m}$, where m = J" + 1 for the R-branch (J" → J"+1), m = -J" for the P-branch (J" → J"-1), and m = J" for the Q-branch (J" → J"). A different equation is needed for the Q-branch of a given transition than for the P and R branches, because of the differences in the $\underline{c}$ and $\underline{d}$ constants. The general equation is

$$\sigma = \sigma_o + am + bm^2 + cm^3 + dm^4 + em^5 + fm^6,$$

where σ_o is the band origin, $a = B'_v + B''_v$, $b = B'_v - B''_v + D''_v - D'_v$, $c = -(2D'_v + 2D''_v - H'_v - H''_v)$, $d = D''_v - D'_v + 3H'_v - 3H''_v$, $e = 3H'_v + 3H''_v$, and $f = H'_v - H''_v$.

For the Q-branch, the line positions are given by

$$\sigma = \sigma_o + J''(J'' + 1)(B'_v - B''_v) + J''^2(J'' + 1)^2(D''_v - D'_v) + \ldots$$

When expressed in this form it becomes clear from comparisons between new observations and calculations which terms are contributing to the errors. From the figures presented of the new data on CO_2, it can be seen that the even terms are most noticeably in error. This demonstrates the sensitivity of the experiment to the difference of constants such as the upper and lower B-values, or inverse moment of inertia, which are nearly the same for each state. The absolute values of the constants come more directly into

the odd terms in the running index m. For an adequate determination, it is thus necessary to use the global approach.

The method employed in obtaining global constants has utilized the observations made at AFGL at high temperature from 1600 to 2500 cm^{-1} in conjunction with high resolution measurements in several other key regions for CO_2. In the bending mode fundamental region (around 15μm) we have used the FTS measurements of Paso et al[16]. In the CO_2 laser region (≈ 10μm) we have incorporated the results of Freed et al[17], Dupre-Maquaire and Pinson[18], and Siemsen et al[19]. At shorter wavelength (≈ 2μm) we have used the high resolution measurements of Maillard et al[20]. In the same region that our interferometer has scanned, additional measurements at high vibration have been supplied to us from electric discharge measurements made by Bailly et al[21]. The band constants obtained from this effort will appear in a forthcoming publication.

Table VIII. Isotopic CO_2 Lines Observed Between 2140 cm^{-1} and 2340 cm^{-1} at 800K

The listings are:

the transition frequency (cm^{-1})

upper vibrational state

lower vibrational state

branch and lower rotational level

isotope code

molecule identification code

observed minus calculated line positions (cm^{-1})

pressures and temperature of CO_2 samples in which line was observed

2142.5435	0	1	1	1	1	0	1	1	0	1	P116D	636	2	.0021	6T800K	
2145.4082	0	1	1	1	1	0	1	1	0	1	P114D	636	2	-.0020	6T800K	
2145.4082	0	2	2	1	1	0	2	2	0	1	P106C	636	2	.0006	6T800K	
2145.5735	0	0	0	1	1	0	0	0	0	1	P122	636	2	.0025	6T800K	
2147.2726	0	1	1	1	1	0	1	1	0	1	P113C	636	2	.0017	6T800K	
2148.1406	0	2	2	1	1	0	2	2	0	1	P104C	636	2	-.0008	6T800K	
2148.2574	0	1	1	1	1	0	1	1	0	1	P112D	636	2	.0003	6T800K	
2148.5085	0	0	0	1	1	0	0	0	0	1	P120	636	2	.0004	6T800K	
2149.4375	0	2	2	1	1	0	2	2	0	1	P103D	636	2	.0009	6T800K	
2150.0942	0	1	1	1	1	0	1	1	0	1	P111C	636	2	.0016	6T800K	
2150.2712	1	0	0	1	1	1	0	0	0	1	P104	636	2	-.0033	6T800K	
2150.5099	1	0	0	1	2	1	0	0	0	2	P104	636	2	-.0001	6T800K	3T800K
2150.8546	0	2	2	1	1	0	2	2	0	1	P102C	636	2	.0003	6T800K	
2151.0818	0	1	1	1	1	0	1	1	0	1	P110D	636	2	-.0004	6T800K	
2151.4217	0	0	0	1	1	0	0	0	0	1	P118	636	2	-.0015	6T800K	
2152.1478	0	2	2	1	1	0	2	2	0	1	P101D	636	2	.0021	6T800K	
2152.8931	0	1	1	1	1	0	1	1	0	1	P109C	636	2	.0005	6T800K	
2153.0275	1	0	0	1	1	1	0	0	0	1	P102	636	2	-.0020	6T800K	
2153.2112	1	0	0	1	2	1	0	0	0	2	P102	636	2	.0003	6T800K	
2153.5456	0	2	2	1	1	0	2	2	0	1	P100C	636	2	-.0006	6T800K	3T800K
2153.8865	0	1	1	1	1	0	1	1	0	1	P108D	636	2	.0013	6T800K	3T800K
2154.3160	0	0	0	1	1	0	0	0	0	1	P116	636	2	-.0005	6T800K	
2154.8337	0	2	2	1	1	0	2	2	0	1	P 99D	636	2	.0005	6T800K	
2155.6693	0	1	1	1	1	0	1	1	0	1	P107C	636	2	-.0017	6T800K	3T800K
2155.7603	1	0	0	1	1	1	0	0	0	1	P100	636	2	-.0014	6T800K	
2155.8904	1	0	0	1	2	1	0	0	0	2	P100	636	2	-.0002	6T800K	
2156.2173	0	2	2	1	1	0	2	2	0	1	P 98C	636	2	.0002	6T800K	
2156.6661	0	1	1	1	1	0	1	1	0	1	P106D	636	2	-.0002	6T800K	3T800K
2157.1878	0	0	0	1	1	0	0	0	0	1	P114	636	2	.0000	6T800K	
2157.4975	0	2	2	1	1	0	2	2	0	1	P 97D	636	2	-.0015	3T800K	
2158.4279	0	1	1	1	1	0	1	1	0	1	P105C	636	2	.0002	6T800K	3T800K
2158.4724	1	0	0	1	1	1	0	0	0	1	P 98	636	2	.0013	3T800K	6T800K
2158.5530	1	0	0	1	2	1	0	0	0	2	P 98	636	2	.0011	6T800K	3T800K
2158.8671	0	2	2	1	1	0	2	2	0	1	P 96C	636	2	.0003	6T800K	3T800K
2159.4253	0	1	1	1	1	0	1	1	0	1	P104D	636	2	-.0001	6T800K	3T800K
2160.0387	0	0	0	1	1	0	0	0	0	1	P112	636	2	.0017	3T800K	
2160.1437	0	2	2	1	1	0	2	2	0	1	P 95D	636	2	.0005	6T800K	
2161.1597	1	0	0	1	1	1	0	0	0	1	P 96	636	2	.0020	3T800K	6T800K
2161.1858	1	0	0	1	2	1	0	0	0	2	P 96	636	2	.0001	6T800K	
2161.4938	0	2	2	1	1	0	2	2	0	1	P 94C	636	2	-.0015	3T800K	
2162.1621	0	1	1	1	1	0	1	1	0	1	P102D	636	2	-.0003	6T800K	
2162.6582	0	0	0	1	1	0	0	0	0	1	P102	638	2	.0015	6T800K	3T800K
2162.7640	0	2	2	1	1	0	2	2	0	1	P 93D	636	2	-.0017	3T800K	6T800K
2163.8014	1	0	0	1	2	1	0	0	0	2	P 94	636	2	.0003	3T800K	
2163.8755	0	1	1	1	1	0	1	1	0	1	P101C	636	2	-.0003	6T800K	3T800K
2163.9395	0	0	0	1	1	0	0	0	0	1	P101	638	2	-.0012	3T800K	6T800K
2164.1002	0	2	2	1	1	0	2	2	0	1	P 92C	636	2	-.0023	3T800K	6T800K
2164.8787	0	1	1	1	1	0	1	1	0	1	P100D	636	2	.0014	3T800K	6T800K
2165.3641	0	2	2	1	1	0	2	2	0	1	P 91D	636	2	-.0023	3T800K	
2165.6698	0	0	0	1	1	0	0	0	0	1	P108	636	2	.0004	3T800K	6T800K

2166.3936	1	0	0	1	2	1	0	0	0	2	P 92	636	2	-.0015	3T800K	6T800K
2166.4650	1	0	0	1	1	1	0	0	0	1	P 92	636	2	.0027	3T800K	6T800K
2166.5674	0	1	1	1	1	0	1	1	0	1	P 99C	638	2	.0002	6T800K	3T800K
2166.6879	0	2	2	1	1	0	2	2	0	1	P 90C	636	2	-.0005	6T800K	
2167.5707	0	1	1	1	1	0	1	1	0	1	P 98D	636	2	.0006	6T800K	3T800K
2167.7596	0	0	0	1	1	0	0	0	0	1	P 98	638	2	-.0015	3T800K	
2167.9445	0	2	2	1	1	0	2	2	0	1	P 89D	636	2	-.0009	6T800K	3T800K
2168.4526	0	0	0	1	1	0	0	0	0	1	P106	636	2	.0001	3T800K	6T800K
2168.9649	1	0	0	1	2	1	0	0	0	2	P 90	636	2	-.0026	3T800K	
2169.0250	0	0	0	1	1	0	0	0	0	1	P 97	638	2	.0009	3T800K	6T800K
2169.0800	1	0	0	1	1	1	0	0	0	1	P 90	636	2	-.0003	6T800K	3T800K
2169.2372	0	1	1	1	1	0	1	1	0	1	P 97C	636	2	.0005	6T800K	3T800K
2169.2545	0	2	2	1	1	0	2	2	0	1	P 88C	636	2	.0017	3T800K	
2170.2401	0	1	1	1	1	0	1	1	0	1	P 96D	636	2	-.0007	6T800K	3T800K
2170.2824	0	0	0	1	1	0	0	0	0	1	P 96	638	2	.0006	6T800K	
2171.2127	0	0	0	1	1	0	0	0	0	1	P104	636	2	-.0008	3T800K	
2171.5185	1	0	0	1	2	1	0	0	0	2	P 88	636	2	.0001	3T800K	6T800K
2171.6747	1	0	0	1	1	1	0	0	0	1	P 88	636	2	-.0007	6T800K	3T800K
2171.7953	0	2	2	1	1	0	2	2	0	1	P 86C	636	2	-.0004	6T800K	
2171.8844	0	1	1	1	1	0	1	1	0	1	P 95C	636	2	.0000	3T800K	
2172.7825	0	0	0	1	1	0	0	0	0	1	P 94	638	2	.0011	6T800K	3T800K
2172.8884	0	1	1	1	1	0	1	1	0	1	P 94D	636	2	-.0008	6T800K	3T800K
2173.0374	0	2	2	1	1	0	2	2	0	1	P 85D	636	2	-.0002	6T800K	3T800K
2173.9520	0	0	0	1	1	0	0	0	0	1	P102	636	2	-.0002	6T800K	3T800K
2174.0232	0	0	0	1	1	0	0	0	0	1	P 93	638	2	.0000	6T800K	3T800K
2174.2477	1	0	0	1	1	1	0	0	0	1	P 86	636	2	.0001	3T800K	
2174.5105	0	1	1	1	1	0	1	1	0	1	P 93C	636	2	.0004	3T800K	6T800K
2175.2602	0	0	0	1	1	0	0	0	0	1	P 92	638	2	.0004	6T800K	3T800K
2175.5156	0	1	1	1	1	0	1	1	0	1	P 92D	636	2	.0001	3T800K	6T800K
2175.5514	0	2	2	1	1	0	2	2	0	1	P 83D	636	2	.0005	3T800K	
2176.4913	0	0	0	1	1	0	0	0	0	1	P 91	638	2	.0002	3T800K	
2176.5553	1	0	0	1	2	1	0	0	0	2	P 84	636	2	.0000	3T800K	6T800K
2176.6696	0	0	0	1	1	0	0	0	0	1	P100	636	2	.0008	6T800K	3T800K
2176.7964	1	0	0	1	1	1	0	0	0	1	P 84	636	2	-.0005	3T800K	
2176.8177	0	2	2	1	1	0	2	2	0	1	P 82C	636	2	.0010	3T800K	
2177.1126	0	1	1	1	1	0	1	1	0	1	P 91C	636	2	-.0012	6T800K	3T800K
2178.0422	0	2	2	1	1	0	2	2	0	1	P 81D	636	2	.0000	3T800K	6T800K
2178.1193	0	1	1	1	1	0	1	1	0	1	P 90D	636	2	-.0001	3T800K	6T800K
2178.9382	0	0	0	1	1	0	0	0	0	1	P 89	638	2	.0004	3T800K	6T800K
2179.0413	1	0	0	1	2	1	0	0	0	2	P 82	636	2	-.0001	3T800K	6T800K
2179.2959	0	2	2	1	1	0	2	2	0	1	P 80C	636	2	.0012	3T800K	6T800K
2179.3212	1	0	0	1	1	1	0	0	0	1	P 82	636	2	-.0020	3T800K	
2179.3648	0	0	0	1	1	0	0	0	0	1	P 98	636	2	.0017	6T800K	3T800K
2180.1524	0	0	0	1	1	0	0	0	0	1	P 88	638	2	-.0008	3T800K	
2180.5119	0	2	2	1	1	0	2	2	0	1	P 79D	636	2	.0004	3T800K	6T800K
2181.3631	0	0	0	1	1	0	0	0	0	1	P 87	638	2	-.0002	3T800K	6T800K
2181.5058	1	0	0	1	2	1	0	0	0	2	P 80	636	2	.0001	3T800K	6T800K
2181.8246	1	0	0	1	1	1	0	0	0	1	P 80	636	2	-.0019	3T800K	6T800K
2182.0354	0	0	0	1	1	0	0	0	0	1	P 96	636	2	.0002	3T800K	6T800K
2182.2550	0	1	1	1	1	0	1	1	0	1	P 87C	636	2	-.0003	3T800K	6T800K

2182.5682	0 0 0 1 1	0 0 0 0 1	P	86	638	2	.0000	3T800K	6T800K
2182.9587	0 2 2 1 1	0 2 2 0 1	P	77D	636	2	-.0001	3T800K	6T800K
2183.2602	0 1 1 1 1	0 1 1 0 1	P	86D	636	2	-.0003	3T800K	6T800K
2183.9486	1 0 0 1 2	1 0 0 0 2	P	78	636	2	.0002	3T800K	
2184.1830	0 2 2 1 1	0 2 2 0 1	P	76C	636	2	-.0023	3T800K	
2184.3081	1 0 0 1 1	1 0 0 0 1	P	78	636	2	.0012	6T800K	3T800K
2184.6860	0 0 0 1 1	0 0 0 0 1	P	94	636	2	.0011	6T800K	3T800K
2184.7902	0 1 1 1 1	0 1 1 0 1	P	85C	636	2	-.0027	6T800K	
2184.9612	0 0 0 1 1	0 0 0 0 1	P	84	638	2	-.0008	3T800K	6T800K
2185.3839	0 2 2 1 1	0 2 2 0 1	P	75D	636	2	-.0001	6T800K	3T800K
2185.7990	0 1 1 1 1	0 1 1 0 1	P	84D	636	2	.0015	6T800K	3T800K
2186.1506	0 0 0 1 1	0 0 0 0 1	P	83	638	2	-.0001	6T800K	3T800K
2186.3688	1 0 0 1 2	1 0 0 0 2	P	76	636	2	-.0005	3T800K	6T800K
2186.5978	0 2 2 1 1	0 2 2 0 1	P	74C	636	2	.0001	3T800K	
2186.7645	1 0 0 1 1	1 0 0 0 1	P	76	636	2	.0003	3T800K	6T800K
2187.3105	0 0 0 1 1	0 0 0 0 1	P	92	636	2	-.0018	3T800K	6T800K
2187.3105	0 1 1 1 1	0 1 1 0 1	P	83C	636	2	.0021	3T800K	
2187.3343	0 0 0 1 1	0 0 0 0 1	P	82	638	2	.0000	3T800K	
2187.7873	0 2 2 1 1	0 2 2 0 1	P	73D	636	2	.0003	6T800K	3T800K
2188.3119	0 1 1 1 1	0 1 1 0 1	P	82D	636	2	-.0003	6T800K	3T800K
2188.7694	1 0 0 1 2	1 0 0 0 2	P	74	636	2	.0010	6T800K	
2188.9878	0 2 2 1 1	0 2 2 0 1	P	72C	636	2	-.0005	6T800K	3T800K
2189.6830	0 0 0 1 1	0 0 0 0 1	P	80	638	2	-.0024	3T800K	
2189.7997	0 1 1 1 1	0 1 1 0 1	P	81C	636	2	-.0020	6T800K	
2189.9165	0 0 0 1 1	0 0 0 0 1	P	90	636	2	-.0009	6T800K	
2190.1684	0 2 2 1 1	0 2 2 0 1	P	71D	636	2	.0005	3T800K	
2190.8029	0 1 1 1 1	0 1 1 0 1	P	80D	636	2	-.0015	6T800K	3T800K
2190.8527	0 0 0 1 1	0 0 0 0 1	P	79	638	2	-.0003	3T800K	6T800K
2191.1448	1 0 0 1 2	1 0 0 0 2	P	72	636	2	-.0009	3T800K	
2191.3585	0 2 2 1 1	0 2 2 0 1	P	70C	636	2	.0017	3T800K	6T800K
2191.6091	1 0 0 1 1	1 0 0 0 1	P	72	636	2	-.0005	3T800K	6T800K
2192.0144	0 0 0 1 1	0 0 0 0 1	P	78	638	2	-.0008	3T800K	6T800K
2192.2714	0 1 1 1 1	0 1 1 0 1	P	79C	636	2	-.0015	6T800K	
2192.5003	0 0 0 1 1	0 0 0 0 1	P	88	636	2	.0003	6T800K	
2192.5266	0 2 2 1 1	0 2 2 0 1	P	69D	636	2	.0000	3T800K	6T800K
2193.1739	0 0 0 1 1	0 0 0 0 1	P	77	638	2	.0018	3T800K	6T800K
2193.2756	0 1 1 1 1	0 1 1 0 1	P	78D	636	2	.0014	6T800K	3T800K
2193.7034	0 2 2 1 1	0 2 2 0 1	P	68C	636	2	.0001	3T800K	6T800K
2193.9990	1 0 0 1 1	1 0 0 0 1	P	70	636	2	.0013	6T800K	3T800K
2194.7205	0 1 1 1 1	0 1 1 0 1	P	77C	636	2	-.0013	6T800K	
2194.8642	0 2 2 1 1	0 2 2 0 1	P	67D	636	2	.0011	6T800K	3T800K
2195.0597	0 0 0 1 1	0 0 0 0 1	P	86	636	2	-.0005	3T800K	6T800K
2195.4702	0 0 0 1 1	0 0 0 0 1	P	75	638	2	.0003	3T800K	6T800K
2195.7221	0 1 1 1 1	0 1 1 0 1	P	76D	636	2	.0006	6T800K	3T800K
2195.8355	1 0 0 1 2	1 0 0 0 2	P	68	636	2	.0009	3T800K	6T800K
2196.0258	0 2 2 1 1	0 2 2 0 1	P	66C	636	2	-.0018	3T800K	
2196.3631	1 0 0 1 1	1 0 0 0 1	P	68	636	2	.0004	6T800K	
2197.1486	0 1 1 1 1	0 1 1 0 1	P	75C	636	2	.0001	3T800K	6T800K
2197.5983	0 0 0 1 1	0 0 0 0 1	P	84	636	2	.0003	6T800K	3T800K
2198.1464	0 1 1 1 1	0 1 1 0 1	P	74D	636	2	.0002	3T800K	6T800K

2198.1464	1 0 0 1 2	1 0 0 0 2	P	66	636	2	.0001	3T800K	6T800K
2198.3305	0 2 2 1 1	0 2 2 0 1	P	64C	636	2	.0007	6T800K	3T800K
2198.7047	1 0 0 1 1	1 0 0 0 1	P	66	636	2	.0001	6T800K	
2198.8781	0 0 0 1 1	0 0 0 0 1	P	72	638	2	.0016	3T800K	6T800K
2199.4689	0 2 2 1 1	0 2 2 0 1	P	63D	636	2	-.0003	6T800K	3T800K
2199.5528	0 1 1 1 1	0 1 1 0 1	P	73C	636	2	-.0001	3T800K	6T800K
2200.1125	0 0 0 1 1	0 0 0 0 1	P	82	636	2	-.0007	3T800K	
2200.4359	1 0 0 1 2	1 0 0 0 2	P	64	636	2	.0000	3T800K	6T800K
2200.5478	0 1 1 1 1	0 1 1 0 1	P	72D	636	2	-.0007	6T800K	3T800K
2200.6110	0 2 2 1 1	0 2 2 0 1	P	62C	636	2	.0012	3T800K	6T800K
2201.0225	1 0 0 1 1	1 0 0 0 1	P	64	636	2	-.0007	3T800K	6T800K
2201.1211	0 0 0 1 1	0 0 0 0 1	P	70	638	2	.0003	6T800K	3T800K
2201.7387	0 2 2 1 1	0 2 2 0 1	P	61D	636	2	.0000	6T800K	3T800K
2201.9364	0 1 1 1 1	0 1 1 0 1	P	71C	636	2	.0015	3T800K	6T800K
2202.2362	0 0 0 1 1	0 0 0 0 1	P	69	638	2	.0013	6T800K	3T800K
2202.6041	0 0 0 1 1	0 0 0 0 1	P	80	636	2	-.0018	6T800K	3T800K
2202.7035	1 0 0 1 2	1 0 0 0 2	P	62	636	2	-.0001	3T800K	6T800K
2202.8667	0 2 2 1 1	0 2 2 0 1	P	60C	636	2	-.0008	3T800K	6T800K
2202.9282	0 1 1 1 1	0 1 1 0 1	P	70D	636	2	.0001	6T800K	3T800K
2203.3197	1 0 0 1 1	1 0 0 0 1	P	62	636	2	.0010	3T800K	6T800K
2203.3455	0 0 0 1 1	0 0 0 0 1	P	68	638	2	.0018	3T800K	6T800K
2203.9863	0 2 2 1 1	0 2 2 0 1	P	59D	636	2	.0005	6T800K	3T800K
2204.2934	0 1 1 1 1	0 1 1 0 1	P	69C	636	2	-.0012	6T800K	3T800K
2204.4470	0 0 0 1 1	0 0 0 0 1	P	67	638	2	.0000	3T800K	6T800K
2204.9494	1 0 0 1 2	1 0 0 0 2	P	60	636	2	.0001	6T800K	3T800K
2205.0754	0 0 0 1 1	0 0 0 0 1	P	78	636	2	-.0006	6T800K	3T800K
2205.1019	0 2 2 1 1	0 2 2 0 1	P	58C	636	2	-.0011	3T800K	6T800K
2205.2848	0 1 1 1 1	0 1 1 0 1	P	68D	636	2	-.0004	6T800K	3T800K
2205.5447	0 0 0 1 1	0 0 0 0 1	P	66	638	2	-.0003	3T800K	
2205.5913	1 0 0 1 1	1 0 0 0 1	P	60	636	2	.0003	3T800K	6T800K
2206.2101	0 2 2 1 1	0 2 2 0 1	P	57D	636	2	-.0005	6T800K	
2206.6355	0 0 0 1 1	0 0 0 0 1	P	65	638	2	-.0021	3T800K	6T800K
2207.1731	1 0 0 1 2	1 0 0 0 2	P	58	636	2	.0003	3T800K	
2207.3167	0 2 2 1 1	0 2 2 0 1	P	56C	636	2	.0007	6T800K	
2207.5236	0 0 0 1 1	0 0 0 0 1	P	76	636	2	.0000	6T800K	3T800K
2207.6207	0 1 1 1 1	0 1 1 0 1	P	66D	636	2	.0011	6T800K	3T800K
2207.7259	0 0 0 1 1	0 0 0 0 1	P	64	638	2	.0010	3T800K	6T800K
2207.8402	1 0 0 1 1	1 0 0 0 1	P	58	636	2	.0001	6T800K	
2208.4135	0 2 2 1 1	0 2 2 0 1	P	55D	636	2	.0007	3T800K	
2208.8055	0 0 0 1 1	0 0 0 0 1	P	63	638	2	-.0012	6T800K	3T800K
2208.9469	0 1 1 1 1	0 1 1 0 1	P	65C	636	2	.0002	3T800K	6T800K
2209.3740	1 0 0 1 2	1 0 0 0 2	P	56	636	2	-.0003	6T800K	
2209.5075	0 2 2 1 1	0 2 2 0 1	P	54C	636	2	.0008	6T800K	3T800K
2209.8839	0 0 0 1 1	0 0 0 0 1	P	62	638	2	.0007	3T800K	6T800K
2209.9315	0 1 1 1 1	0 1 1 0 1	P	64D	636	2	.0001	6T800K	
2209.9480	0 0 0 1 1	0 0 0 0 1	P	74	636	2	-.0005	6T800K	3T800K
2210.0662	1 0 0 1 1	1 0 0 0 1	P	56	636	2	.0003	6T800K	3T800K
2210.5927	0 2 2 1 1	0 2 2 0 1	P	53D	636	2	.0001	3T800K	6T800K
2210.9544	0 0 0 1 1	0 0 0 0 1	P	61	638	2	.0001	6T800K	3T800K
2211.2392	0 1 1 1 1	0 1 1 0 1	P	63C	636	2	.0002	3T800K	6T800K

2211.5538	1 0 0 1 2	1 0 0 0 2	P	54	636	2	.0001	6T800K	3T800K
2211.6738	0 2 2 1 1	0 2 2 0 1	P	52C	636	2	-.0011	6T800K	3T800K
2212.0198	0 0 0 1 1	0 0 0 0 1	P	60	638	2	-.0002	6T800K	3T800K
2212.2203	0 1 1 1 1	0 1 1 0 1	P	62D	636	2	-.0001	6T800K	3T800K
2212.2684	1 0 0 1 1	1 0 0 0 1	P	54	636	2	.0000	3T800K	
2212.3504	0 0 0 1 1	0 0 0 0 1	P	72	636	2	-.0003	3T800K	
2212.7499	0 2 2 1 1	0 2 2 0 1	P	51D	636	2	.0000	6T800K	3T800K
2213.0804	0 0 0 1 1	0 0 0 0 1	P	59	638	2	.0001	3T800K	6T800K
2213.5105	0 1 1 1 1	0 1 1 0 1	P	61C	636	2	.0016	3T800K	
2213.7110	1 0 0 1 2	1 0 0 0 2	P	52	636	2	.0001	6T800K	3T800K
2213.8193	0 2 2 1 1	0 2 2 0 1	P	50C	636	2	-.0014	3T800K	6T800K
2214.1339	0 0 0 1 1	0 0 0 0 1	P	58	638	2	-.0013	6T800K	3T800K
2214.4484	1 0 0 1 1	1 0 0 0 1	P	52	636	2	.0007	6T800K	
2214.4868	0 1 1 1 1	0 1 1 0 1	P	60D	636	2	.0001	3T800K	6T800K
2214.7288	0 0 0 1 1	0 0 0 0 1	P	70	636	2	-.0015	6T800K	
2214.8845	0 2 2 1 1	0 2 2 0 1	P	49D	636	2	-.0001	3T800K	6T800K
2215.1845	0 0 0 1 1	0 0 0 0 1	P	57	638	2	-.0001	3T800K	
2215.7566	0 1 1 1 1	0 1 1 0 1	P	59C	636	2	.0004	3T800K	
2215.8465	1 0 0 1 2	1 0 0 0 2	P	50	636	2	.0006	6T800K	3T800K
2215.9437	0 2 2 1 1	0 2 2 0 1	P	48C	636	2	-.0002	3T800K	
2216.2287	0 0 0 1 1	0 0 0 0 1	P	56	638	2	.0000	6T800K	3T800K
2216.6033	1 0 0 1 1	1 0 0 0 1	P	50	636	2	-.0003	3T800K	
2216.7313	0 1 1 1 1	0 1 1 0 1	P	58D	636	2	.0010	3T800K	
2216.9968	0 2 2 1 1	0 2 2 0 1	P	47D	636	2	.0001	3T800K	6T800K
2217.0873	0 0 0 1 1	0 0 0 0 1	P	68	636	2	.0002	3T800K	6T800K
2217.2678	0 0 0 1 1	0 0 0 0 1	P	55	638	2	.0004	3T800K	
2217.9589	1 0 0 1 2	1 0 0 0 2	P	48	636	2	.0002	3T800K	6T800K
2217.9812	0 1 1 1 1	0 1 1 0 1	P	57C	636	2	.0003	3T800K	6T800K
2218.0446	0 2 2 1 1	0 2 2 0 1	P	46C	636	2	.0001	6T800K	3T800K
2218.3007	0 0 0 1 1	0 0 0 0 1	P	54	638	2	.0000	6T800K	3T800K
2218.7360	1 0 0 1 1	1 0 0 0 1	P	48	636	2	-.0001	3T800K	
2218.9506	0 1 1 1 1	0 1 1 0 1	P	56D	636	2	-.0004	6T800K	3T800K
2219.0864	0 2 2 1 1	0 2 2 0 1	P	45D	636	2	.0002	6T800K	3T800K
2219.3287	0 0 0 1 1	0 0 0 0 1	P	53	638	2	.0002	6T800K	3T800K
2219.4215	0 0 0 1 1	0 0 0 0 1	P	66	636	2	.0003	3T800K	
2220.0494	1 0 0 1 2	1 0 0 0 2	P	46	636	2	.0002	6T800K	3T800K
2220.1220	0 2 2 1 1	0 2 2 0 1	P	44C	636	2	-.0005	3T800K	
2220.1830	0 1 1 1 1	0 1 1 0 1	P	55C	636	2	.0000	6T800K	3T800K
2220.3501	0 0 0 1 1	0 0 0 0 1	P	52	638	2	-.0008	6T800K	3T800K
2220.8435	1 0 0 1 1	1 0 0 0 1	P	46	636	2	-.0018	3T800K	6T800K
2221.1500	0 1 1 1 1	0 1 1 0 1	P	54D	636	2	.0010	6T800K	3T800K
2221.3688	0 0 0 1 1	0 0 0 0 1	P	51	638	2	.0009	6T800K	3T800K
2221.7328	0 0 0 1 1	0 0 0 0 1	P	64	636	2	.0003	3T800K	6T800K
2222.1173	1 0 0 1 2	1 0 0 0 2	P	44	636	2	-.0002	3T800K	6T800K
2222.1773	0 2 2 1 1	0 2 2 0 1	P	42C	636	2	-.0006	3T800K	6T800K
2222.3631	0 1 1 1 1	0 1 1 0 1	P	53C	636	2	.0006	3T800K	
2222.9308	1 0 0 1 1	1 0 0 0 1	P	44	636	2	-.0002	6T800K	3T800K
2223.1968	0 2 2 1 1	0 2 2 0 1	P	41D	636	2	-.0003	3T800K	6T800K
2223.3236	0 1 1 1 1	0 1 1 0 1	P	52D	636	2	-.0005	3T800K	6T800K
2223.3874	0 0 0 1 1	0 0 0 0 1	P	49	638	2	.0017	3T800K	6T800K

2224.0212	0 0 0 1 1	0 0 0 0 1	P	62	636	2	.0002	3T800K	
2224.1631	1 0 0 1 2	1 0 0 0 2	P	42	636	2	-.0002	6T800K	3T800K
2224.2125	0 2 2 1 1	0 2 2 0 1	P	40C	636	2	.0019	6T800K	3T800K
2224.3866	0 0 0 1 1	0 0 0 0 1	P	48	638	2	.0002	6T800K	
2224.5197	0 1 1 1 1	0 1 1 0 1	P	51C	636	2	.0004	3T800K	
2224.9934	1 0 0 1 1	1 0 0 0 1	P	42	636	2	.0000	3T800K	6T800K
2225.2180	0 2 2 1 1	0 2 2 0 1	P	39D	636	2	-.0005	6T800K	3T800K
2225.3814	0 0 0 1 1	0 0 0 0 1	P	47	638	2	-.0003	3T800K	
2225.4764	0 1 1 1 1	0 1 1 0 1	P	50D	636	2	.0001	3T800K	
2226.1866	1 0 0 1 2	1 0 0 0 2	P	40	636	2	-.0003	3T800K	
2226.2206	0 2 2 1 1	0 2 2 0 1	P	38C	636	2	.0000	3T800K	6T800K
2226.2873	0 0 0 1 1	0 0 0 0 1	P	60	636	2	.0007	3T800K	6T800K
2226.3716	0 0 0 1 1	0 0 0 0 1	P	46	638	2	.0001	6T800K	3T800K
2226.6535	0 1 1 1 1	0 1 1 0 1	P	49C	636	2	.0001	3T800K	6T800K
2227.0307	1 0 0 1 1	1 0 0 0 1	P	40	636	2	-.0016	3T800K	
2227.2174	0 2 2 1 1	0 2 2 0 1	P	37D	636	2	.0002	3T800K	
2227.3559	0 0 0 1 1	0 0 0 0 1	P	45	638	2	.0000	3T800K	6T800K
2227.6052	0 1 1 1 1	0 1 1 0 1	P	48D	636	2	-.0004	3T800K	6T800K
2228.1880	1 0 0 1 2	1 0 0 0 2	P	38	636	2	.0000	3T800K	6T800K
2228.2069	0 2 2 1 1	0 2 2 0 1	P	36C	636	2	-.0010	3T800K	6T800K
2228.3353	0 0 0 1 1	0 0 0 0 1	P	44	638	2	.0004	6T800K	3T800K
2228.5298	0 0 0 1 1	0 0 0 0 1	P	58	636	2	.0004	3T800K	
2228.7652	0 1 1 1 1	0 1 1 0 1	P	47C	636	2	.0004	6T800K	3T800K
2229.0479	1 0 0 1 1	1 0 0 0 1	P	38	636	2	.0002	3T800K	
2229.1935	0 2 2 1 1	0 2 2 0 1	P	35D	636	2	.0004	6T800K	
2229.3076	0 0 0 1 1	0 0 0 0 1	P	43	638	2	-.0008	6T800K	3T800K
2229.7125	0 1 1 1 1	0 1 1 0 1	P	46D	636	2	.0006	3T800K	
2230.1689	1 0 0 1 2	1 0 0 0 2	P	36	636	2	.0022	6T800K	3T800K
2230.2766	0 0 0 1 1	0 0 0 0 1	P	42	638	2	.0002	3T800K	6T800K
2230.7495	0 0 0 1 1	0 0 0 0 1	P	56	636	2	.0002	3T800K	
2230.8533	0 1 1 1 1	0 1 1 0 1	P	45C	636	2	-.0001	3T800K	
2231.0396	1 0 0 1 1	1 0 0 0 1	P	36	636	2	.0000	3T800K	
2231.1463	0 2 2 1 1	0 2 2 0 1	P	33D	636	2	.0002	3T800K	
2231.2388	0 0 0 1 1	0 0 0 0 1	P	41	638	2	-.0002	3T800K	6T800K
2231.7954	0 1 1 1 1	0 1 1 0 1	P	44D	636	2	.0001	3T800K	
2232.1963	0 0 0 1 1	0 0 0 0 1	P	40	638	2	.0001	6T800K	3T800K
2232.9195	0 1 1 1 1	0 1 1 0 1	P	43C	636	2	.0003	3T800K	
2232.9463	0 0 0 1 1	0 0 0 0 1	P	54	636	2	.0001	3T800K	
2233.0064	1 0 0 1 1	1 0 0 0 1	P	34	636	2	-.0016	3T800K	6T800K
2233.0764	0 2 2 1 1	0 2 2 0 1	P	31D	636	2	.0001	3T800K	6T800K
2233.1480	0 0 0 1 1	0 0 0 0 1	P	39	638	2	.0001	6T800K	
2233.8547	0 1 1 1 1	0 1 1 0 1	P	42D	636	2	-.0010	3T800K	6T800K
2234.0324	0 2 2 1 1	0 2 2 0 1	P	30C	636	2	-.0003	3T800K	6T800K
2234.0561	1 0 0 1 2	1 0 0 0 2	P	32	636	2	-.0006	6T800K	3T800K
2234.0942	0 0 0 1 1	0 0 0 0 1	P	38	638	2	.0001	3T800K	6T800K
2234.9828	0 2 2 1 1	0 2 2 0 1	P	29D	636	2	-.0003	6T800K	3T800K
2235.0350	0 0 0 1 1	0 0 0 0 1	P	37	638	2	.0001	6T800K	3T800K
2235.1204	0 0 0 1 1	0 0 0 0 1	P	52	636	2	.0002	3T800K	
2235.8929	0 1 1 1 1	0 1 1 0 1	P	40D	636	2	-.0001	3T800K	6T800K
2235.9284	0 2 2 1 1	0 2 2 0 1	P	28C	636	2	-.0001	6T800K	3T800K

2235.9683	1 0 0 1 2	1 0 0 0 2	P	30	636	2	.0004	3T800K	
2235.9688	0 0 0 1 1	0 0 0 0 1	P	36	638	2	-.0013	6T800K	3T800K
2236.8685	0 2 2 1 1	0 2 2 0 1	P	27D	636	2	.0005	3T800K	
2236.9819	0 1 1 1 1	0 1 1 0 1	P	39C	636	2	-.0003	3T800K	6T800K
2237.2715	0 0 0 1 1	0 0 0 0 1	P	50	636	2	.0004	3T800K	
2237.8019	0 2 2 1 1	0 2 2 0 1	P	26C	636	2	.0004	6T800K	3T800K
2237.8242	0 0 0 1 1	0 0 0 0 1	P	34	638	2	-.0001	3T800K	6T800K
2237.8566	1 0 0 1 2	1 0 0 0 2	P	28	636	2	.0001	3T800K	
2237.9072	0 1 1 1 1	0 1 1 0 1	P	38D	636	2	-.0001	3T800K	6T800K
2238.7718	1 0 0 1 1	1 0 0 0 1	P	28	636	2	-.0001	3T800K	6T800K
2238.9787	0 1 1 1 1	0 1 1 0 1	P	37C	636	2	-.0007	3T800K	6T800K
2239.4004	0 0 0 1 1	0 0 0 0 1	P	48	636	2	.0014	3T800K	
2239.6536	0 2 2 1 1	0 2 2 0 1	P	24C	636	2	.0021	6T800K	3T800K
2239.7217	1 0 0 1 2	1 0 0 0 2	P	26	636	2	-.0008	3T800K	6T800K
2239.8983	0 1 1 1 1	0 1 1 0 1	P	36D	636	2	-.0002	3T800K	6T800K
2240.5651	0 0 0 1 1	0 0 0 0 1	P	31	638	2	.0007	6T800K	
2240.5660	0 2 2 1 1	0 2 2 0 1	P	23D	636	2	-.0020	3T800K	
2240.6463	1 0 0 1 1	1 0 0 0 1	P	26	636	2	.0004	3T800K	6T800K
2240.9531	0 1 1 1 1	0 1 1 0 1	P	35C	636	2	-.0005	3T800K	
2241.5038	0 0 0 1 1	0 0 0 0 1	P	46	636	2	-.0001	3T800K	
2241.5658	1 0 0 1 2	1 0 0 0 2	P	24	636	2	-.0001	3T800K	
2241.8665	0 1 1 1 1	0 1 1 0 1	P	34D	636	2	-.0001	3T800K	6T800K
2242.3643	0 0 0 1 1	0 0 0 0 1	P	29	638	2	.0006	3T800K	6T800K
2242.3835	0 2 2 1 1	0 2 2 0 1	P	21D	636	2	.0000	3T800K	
2242.4962	1 0 0 1 1	1 0 0 0 1	P	24	636	2	-.0002	3T800K	6T800K
2242.9050	0 1 1 1 1	0 1 1 0 1	P	33C	636	2	.0001	3T800K	
2243.2558	0 0 0 1 1	0 0 0 0 1	P	28	638	2	.0006	6T800K	3T800K
2243.2823	0 2 2 1 1	0 2 2 0 1	P	20C	636	2	-.0002	3T800K	6T800K
2243.3854	1 0 0 1 2	1 0 0 0 2	P	22	636	2	-.0013	6T800K	3T800K
2243.5859	0 0 0 1 1	0 0 0 0 1	P	44	636	2	.0002	3T800K	
2243.8115	0 1 1 1 1	0 1 1 0 1	P	32D	636	2	-.0001	3T800K	
2244.1408	0 0 0 1 1	0 0 0 0 1	P	27	638	2	-.0003	3T800K	
2244.1764	0 2 2 1 1	0 2 2 0 1	P	19D	636	2	.0005	3T800K	
2244.3248	1 0 0 1 1	1 0 0 0 1	P	22	636	2	.0017	3T800K	6T800K
2244.8333	0 1 1 1 1	0 1 1 0 1	P	31C	636	2	.0001	3T800K	6T800K
2245.0214	0 0 0 1 1	0 0 0 0 1	P	26	638	2	-.0001	6T800K	3T800K
2245.0632	0 2 2 1 1	0 2 2 0 1	P	18C	636	2	-.0002	3T800K	
2245.6445	0 0 0 1 1	0 0 0 0 1	P	42	636	2	.0001	3T800K	
2245.7332	0 1 1 1 1	0 1 1 0 1	P	30D	636	2	-.0001	3T800K	
2245.8967	0 0 0 1 1	0 0 0 0 1	P	25	638	2	.0003	6T800K	3T800K
2245.9475	0 2 2 1 1	0 2 2 0 1	P	17D	636	2	.0022	3T800K	6T800K
2246.1266	1 0 0 1 1	1 0 0 0 1	P	20	636	2	.0004	6T800K	3T800K
2246.7393	0 1 1 1 1	0 1 1 0 1	P	29C	636	2	.0008	3T800K	
2246.7643	0 0 0 1 1	0 0 0 0 1	P	24	638	2	-.0015	3T800K	6T800K
2246.8218	0 2 2 1 1	0 2 2 0 1	P	16C	636	2	.0006	6T800K	3T800K
2246.9598	1 0 0 1 2	1 0 0 0 2	P	18	636	2	-.0003	6T800K	3T800K
2247.6307	0 0 0 1 1	0 0 0 0 1	P	23	638	2	.0010	3T800K	
2247.6313	0 1 1 1 1	0 1 1 0 1	P	28D	636	2	-.0006	3T800K	6T800K
2247.6805	0 0 0 1 1	0 0 0 0 1	P	40	636	2	.0006	3T800K	
2247.6893	0 2 2 1 1	0 2 2 0 1	P	15D	636	2	-.0023	6T800K	

2247.9049	1 0 0 . 1	1 0 0 0 1	P 18	636	2	-.0007	3T800K	6T800K				
2248.4872	0 0 0 1 1	0 0 0 0 1	P 22	638	2	-.0009	6T800K	3T800K				
2248.5560	0 2 2 1 1	0 2 2 0 1	P 14C	636	2	.0000	3T800K	6T800K				
2248.6205	0 1 1 1 1	0 1 1 0 1	P 27C	636	2	-.0003	3T800K					
2248.7124	1 0 0 1 2	1 0 0 0 2	P 16	636	2	-.0002	6T800K	3T800K				
2249.3407	0 0 0 1 1	0 0 0 0 1	P 21	638	2	-.0003	3T800K					
2249.4148	0 2 2 1 1	0 2 2 0 1	P 13D	636	2	.0000	3T800K					
2249.5077	0 1 1 1 1	0 1 1 0 1	P 26D	636	2	.0005	3T800K					
2249.6617	1 0 0 1 1	1 0 0 0 1	P 16	636	2	.0005	3T800K					
2249.6906	0 0 0 1 1	0 0 0 0 1	P 38	636	2	-.0017	3T800K					
2250.1882	0 0 0 1 1	0 0 0 0 1	P 20	638	2	-.0001	3T800K					
2250.2676	0 2 2 1 1	0 2 2 0 1	P 12C	636	2	.0000	3T800K	6T800K				
2250.4429	1 0 0 1 2	1 0 0 0 2	P 14	636	2	.0005	6T800K	3T800K				
2250.4799	0 1 1 1 1	0 1 1 0 1	P 25C	636	2	.0000	3T800K					
2251.0303	0 0 0 1 1	0 0 0 0 1	P 19	638	2	.0001	3T800K	6T800K				
2251.1148	0 2 2 1 1	0 2 2 0 1	P 11D	636	2	.0000	3T800K					
2251.3596	0 1 1 1 1	0 1 1 0 1	P 24D	636	2	.0003	3T800K					
2251.3935	1 0 0 1 1	1 0 0 0 1	P 14	636	2	.0005	6T800K	3T800K				
2251.6810	0 0 0 1 1	0 0 0 0 1	P 36	636	2	-.0005	3T800K					
2251.8664	0 0 0 1 1	0 0 0 0 1	P 18	638	2	-.0001	3T800K					
2251.9560	0 2 2 1 1	0 2 2 0 1	P 10C	636	2	-.0001	3T800K					
2252.1493	1 0 0 1 2	1 0 0 0 2	P 12	636	2	-.0001	3T800K					
2252.3155	0 1 1 1 1	0 1 1 0 1	P 23C	636	2	-.0005	3T800K					
2252.6976	0 0 0 1 1	0 0 0 0 1	P 17	638	2	.0003	6T800K					
2252.7913	0 2 2 1 1	0 2 2 0 1	P 9D	636	2	-.0004	3T800K	6T800K				
2253.1018	1 0 0 1 1	1 0 0 0 1	P 12	636	2	.0007	6T800K	3T800K				
2253.1880	0 1 1 1 1	0 1 1 0 1	P 22D	636	2	-.0001	3T800K					
2253.5230	0 0 0 1 1	0 0 0 0 1	P 16	638	2	.0005	3T800K	6T800K				
2253.6476	0 0 0 1 1	0 0 0 0 1	P 34	636	2	.0002	3T800K					
2253.8330	1 0 0 1 2	1 0 0 0 2	P 10	636	2	-.0005	6T800K	3T800K				
2254.1284	0 1 1 1 1	0 1 1 0 1	P 21C	636	2	-.0005	3T800K					
2254.3416	0 0 0 1 1	0 0 0 0 1	P 15	638	2	-.0006	3T800K	6T800K				
2254.4440	0 2 2 1 1	0 2 2 0 1	P 7D	636	2	-.0014	6T800K	3T800K				
2254.7851	1 0 0 1 1	1 0 0 0 1	P 10	636	2	-.0002	3T800K					
2254.9935	0 1 1 1 1	0 1 1 0 1	P 20D	636	2	-.0001	3T800K					
2255.1578	0 0 0 1 1	0 0 0 0 1	P 14	638	2	.0014	3T800K	6T800K				
2255.2647	0 2 2 1 1	0 2 2 0 1	P 6C	636	2	.0013	3T800K	6T800K				
2255.4948	1 0 0 1 2	1 0 0 0 2	P 8	636	2	.0001	3T800K					
2255.5903	0 0 0 1 1	0 0 0 0 1	P 32	636	2	.0002	3T800K					
2255.9178	0 1 1 1 1	0 1 1 0 1	P 19C	636	2	-.0008	3T800K	6T800K				
2255.9649	0 0 0 1 1	0 0 0 0 1	P 13	638	2	-.0001	6T800K	3T800K				
2256.0751	0 2 2 1 1	0 2 2 0 1	P 5D	636	2	-.0007	6T800K	3T800K				
2256.4457	1 0 0 1 1	1 0 0 0 1	P 8	636	2	-.0001	6T800K					
2256.7746	0 1 1 1 1	0 1 1 0 1	P 18D	636	2	-.0012	6T800K					
2256.8811	0 2 2 1 1	0 2 2 0 1	P 4C	636	2	-.0011	6T800K	3T800K				
2257.1333	1 0 0 1 2	1 0 0 0 2	P 6	636	2	.0003	6T800K	3T800K				
2257.5095	0 0 0 1 1	0 0 0 0 1	P 30	636	2	.0000	3T800K					
2257.5656	0 0 0 1 1	0 0 0 0 1	P 11	638	2	-.0001	3T800K					
2257.6851	0 2 2 1 1	0 2 2 0 1	P 3D	636	2	.0021	3T800K	6T800K				
2257.6853	0 1 1 1 1	0 1 1 0 1	P 17C	636	2	.0001	3T800K					

2258.0825	1 0 0 1 1	1 0 0 0 1	P	6	636	2	.0002	6T800K	
2258.3571	0 0 0 1 1	0 0 0 0 1	P	10	638	2	-.0006	6T800K	3T800K
2258.5349	0 1 1 1 1	0 1 1 0 1	P	16D	636	2	.0004	3T800K	
2258.7483	1 0 0 1 2	1 0 0 0 2	P	4	636	2	-.0001	3T800K	
2259.1439	0 0 0 1 1	0 0 0 0 1	P	9	638	2	-.0002	6T800K	3T800K
2259.4066	0 0 0 1 1	0 0 0 0 1	P	28	636	2	.0010	3T800K	
2259.4271	0 1 1 1 1	0 1 1 0 1	P	15C	636	2	-.0014	3T800K	
2259.6950	1 0 0 1 1	1 0 0 0 1	P	4	636	2	.0000	3T800K	6T800K
2259.9265	0 0 0 1 1	0 0 0 0 1	P	8	638	2	.0015	6T800K	3T800K
2260.2691	0 1 1 1 1	0 1 1 0 1	P	14D	636	2	-.0008	3T800K	
2260.3406	1 0 0 1 2	1 0 0 0 2	P	2	636	2	-.0002	3T800K	6T800K
2260.7005	0 0 0 1 1	0 0 0 0 1	P	7	638	2	.0001	3T800K	6T800K
2261.1484	0 1 1 1 1	0 1 1 0 1	P	13C	636	2	-.0002	3T800K	
2261.2773	0 0 0 1 1	0 0 0 0 1	P	26	636	2	-.0010	3T800K	
2261.2857	1 0 0 1 1	1 0 0 0 1	P	2	636	2	.0019	6T800K	
2261.4677	0 0 0 1 1	0 0 0 0 1	P	6	638	2	-.0024	3T800K	
2261.9817	0 1 1 1 1	0 1 1 0 1	P	12D	636	2	-.0002	3T800K	
2262.2349	0 0 0 1 1	0 0 0 0 1	P	5	638	2	.0005	6T800K	
2262.3641	0 2 2 1 1	0 2 2 0 1	R	2C	636	2	-.0005	3T800K	6T800K
2262.6864	1 0 0 1 2	1 0 0 0 2	R	0	636	2	.0001	6T800K	3T800K
2262.8442	0 1 1 1 1	0 1 1 0 1	P	11C	636	2	-.0012	3T800K	
2262.9907	0 0 0 1 1	0 0 0 0 1	P	4	638	2	-.0023	3T800K	
2263.1250	0 2 2 1 1	0 2 2 0 1	R	3D	636	2	.0004	6T800K	3T800K
2263.1254	0 0 0 1 1	0 0 0 0 1	P	24	636	2	-.0023	6T800K	
2263.6703	0 1 1 1 1	0 1 1 0 1	P	10D	636	2	-.0001	3T800K	
2263.7465	0 0 0 1 1	0 0 0 0 1	P	3	638	2	.0004	6T800K	
2263.8785	0 2 2 1 1	0 2 2 0 1	R	4C	636	2	.0000	3T800K	6T800K
2264.2227	1 0 0 1 2	1 0 0 0 2	R	2	636	2	.0016	6T800K	3T800K
2264.4944	0 0 0 1 1	0 0 0 0 1	P	2	638	2	.0008	3T800K	6T800K
2264.5182	0 1 1 1 1	0 1 1 0 1	P	9C	636	2	-.0007	3T800K	
2264.6266	0 2 2 1 1	0 2 2 0 1	R	5D	636	2	-.0002	3T800K	6T800K
2264.9539	0 0 0 1 1	0 0 0 0 1	P	22	636	2	.0002	3T800K	
2265.1507	1 0 0 1 1	1 0 0 0 1	R	2	636	2	-.0002	3T800K	6T800K
2265.2332	0 0 0 1 1	0 0 0 0 1	P	1	638	2	-.0023	6T800K	3T800K
2265.3362	0 1 1 1 1	0 1 1 0 1	P	8D	636	2	.0008	6T800K	3T800K
2265.3690	0 2 2 1 1	0 2 2 0 1	R	6C	636	2	-.0001	3T800K	
2265.7323	1 0 0 1 2	1 0 0 0 2	R	4	636	2	-.0005	6T800K	3T800K
2266.1051	0 2 2 1 1	0 2 2 0 1	R	7D	636	2	-.0005	3T800K	6T800K
2266.1694	0 1 1 1 1	0 1 1 0 1	P	7C	636	2	.0003	6T800K	3T800K
2266.6549	1 0 0 1 1	1 0 0 0 1	R	4	636	2	-.0010	3T800K	6T800K
2266.7032	0 0 0 1 1	0 0 0 0 1	R	0	638	2	.0005	3T800K	
2266.7547	0 0 0 1 1	0 0 0 0 1	P	20	636	2	-.0016	3T800K	
2266.8363	0 2 2 1 1	0 2 2 0 1	R	8C	636	2	.0001	3T800K	6T800K
2266.9771	0 1 1 1 1	0 1 1 0 1	P	6D	636	2	.0002	3T800K	6T800K
2267.2213	1 0 0 1 2	1 0 0 0 2	R	6	636	2	-.0002	3T800K	
2267.4285	0 0 0 1 1	0 0 0 0 1	R	1	638	2	.0006	6T800K	3T800K
2267.5628	0 2 2 1 1	0 2 2 0 1	R	9D	636	2	.0018	6T800K	
2267.7959	0 1 1 1 1	0 1 1 0 1	P	5C	636	2	.0000	3T800K	
2268.2810	0 2 2 1 1	0 2 2 0 1	R	10C	636	2	.0011	3T800K	6T800K
2268.5342	0 0 0 1 1	0 0 0 0 1	P	18	636	2	-.0012	3T800K	

2268.5936	0 1 1 1 1	0 1 1 0 1	P	4D	636	2	-.0013	6T800K	
2268.6869	1 0 0 1 2	1 0 0 0 2	R	8	636	2	-.0001	6T800K	
2268.8610	0 0 0 1 1	0 0 0 0 1	R	3	638	2	-.0005	3T800K	6T800K
2268.9937	0 2 2 1 1	0 2 2 0 1	R	11D	636	2	.0008	3T800K	6T800K
2269.3996	0 1 1 1 1	0 1 1 0 1	P	3C	636	2	.0003	3T800K	
2269.5705	0 0 0 1 1	0 0 0 0 1	R	4	638	2	.0006	3T800K	6T800K
2269.5934	1 0 0 1 1	1 0 0 0 1	R	8	636	2	-.0003	3T800K	
2269.7001	0 2 2 1 1	0 2 2 0 1	R	12C	636	2	.0000	3T800K	6T800K
2270.1291	1 0 0 1 2	1 0 0 0 2	R	10	636	2	-.0002	3T800K	
2270.1896	0 1 1 1 1	0 1 1 0 1	P	2D	636	2	.0003	6T800K	3T800K
2270.2735	0 0 0 1 1	0 0 0 0 1	R	5	638	2	.0007	6T800K	
2270.2927	0 0 0 1 1	0 0 0 0 1	P	16	636	2	.0017	3T800K	
2270.4029	0 2 2 1 1	0 2 2 0 1	R	13D	636	2	.0016	3T800K	6T800K
2270.9699	0 0 0 1 1	0 0 0 0 1	R	6	638	2	-.0001	6T800K	3T800K
2271.0243	1 0 0 1 1	1 0 0 0 1	R	10	636	2	-.0022	3T800K	6T800K
2271.0971	0 2 2 1 1	0 2 2 0 1	R	14C	636	2	.0002	3T800K	
2271.5484	1 0 0 1 2	1 0 0 0 2	R	12	636	2	.0000	3T800K	6T800K
2271.6614	0 0 0 1 1	0 0 0 0 1	R	7	638	2	-.0003	3T800K	6T800K
2271.7868	0 2 2 1 1	0 2 2 0 1	R	15D	636	2	.0005	3T800K	
2272.0232	0 0 0 1 1	0 0 0 0 1	P	14	636	2	.0001	3T800K	
2272.3484	0 0 0 1 1	0 0 0 0 1	R	8	638	2	.0007	6T800K	3T800K
2272.4353	1 0 0 1 1	1 0 0 0 1	R	12	636	2	.0000	6T800K	3T800K
2272.4702	0 2 2 1 1	0 2 2 0 1	R	16C	636	2	.0000	3T800K	6T800K
2272.9448	1 0 0 1 2	1 0 0 0 2	R	14	636	2	.0005	3T800K	6T800K
2273.0281	0 0 0 1 1	0 0 0 0 1	R	9	638	2	.0000	3T800K	6T800K
2273.1478	0 2 2 1 1	0 2 2 0 1	R	17D	636	2	.0001	3T800K	
2273.3068	0 1 1 1 1	0 1 1 0 1	R	1C	636	2	.0015	6T800K	3T800K
2273.7031	0 0 0 1 1	0 0 0 0 1	R	10	638	2	.0001	3T800K	
2273.7337	0 0 0 1 1	0 0 0 0 1	P	12	636	2	.0020	3T800K	
2273.8199	0 2 2 1 1	0 2 2 0 1	R	18C	636	2	-.0001	3T800K	
2273.8199	1 0 0 1 1	1 0 0 0 1	R	14	636	2	.0000	3T800K	
2274.0728	0 1 1 1 1	0 1 1 0 1	R	2D	636	2	.0006	6T800K	3T800K
2274.3159	1 0 0 1 2	1 0 0 0 2	R	16	636	2	-.0011	6T800K	3T800K
2274.3719	0 0 0 1 1	0 0 0 0 1	R	11	638	2	-.0003	3T800K	
2274.4849	0 2 2 1 1	0 2 2 0 1	R	19D	636	2	-.0007	3T800K	6T800K
2274.8257	0 1 1 1 1	0 1 1 0 1	R	3C	636	2	-.0010	3T800K	6T800K
2275.0356	0 0 0 1 1	0 0 0 0 1	R	12	638	2	-.0002	3T800K	
2275.1459	0 2 2 1 1	0 2 2 0 1	R	20C	636	2	-.0003	6T800K	3T800K
2275.1803	1 0 0 1 1	1 0 0 0 1	R	16	636	2	-.0001	6T800K	3T800K
2275.4144	0 0 0 1 1	0 0 0 0 1	P	10	636	2	-.0024	3T800K	
2275.6667	1 0 0 1 2	1 0 0 0 2	R	18	636	2	.0003	3T800K	6T800K
2275.6933	0 0 0 1 1	0 0 0 0 1	R	13	638	2	-.0005	6T800K	3T800K
2275.8000	0 2 2 1 1	0 2 2 0 1	R	21D	636	2	.0001	3T800K	6T800K
2276.3246	0 1 1 1 1	0 1 1 0 1	R	5C	636	2	.0000	3T800K	
2276.3451	0 0 0 1 1	0 0 0 0 1	R	14	638	2	-.0010	3T800K	
2276.4487	0 2 2 1 1	0 2 2 0 1	R	22C	636	2	-.0001	3T800K	6T800K
2276.5171	1 0 0 1 1	1 0 0 0 1	R	18	636	2	.0003	6T800K	3T800K
2276.9926	1 0 0 1 2	1 0 0 0 2	R	20	636	2	.0002	3T800K	
2276.9926	0 0 0 1 1	0 0 0 0 1	R	15	638	2	-.0003	3T800K	
2277.0792	0 0 0 1 1	0 0 0 0 1	P	8	636	2	.0010	3T800K	6T800K

2277.6341	0 0 0 1 1	0 0 0 0 1	R	16	638	2	.0001	6T800K	
2277.7279	0 2 2 1 1	0 2 2 0 1	R	24C	636	2	.0000	3T800K	6T800K
2277.7986	0 1 1 1 1	0 1 1 0 1	R	7C	636	2	-.0003	3T800K	
2277.8300	1 0 0 1 1	1 0 0 0 1	R	20	636	2	.0009	3T800K	6T800K
2278.2700	0 0 0 1 1	0 0 0 0 1	R	17	638	2	.0005	6T800K	3T800K
2278.2944	1 0 0 1 2	1 0 0 0 2	R	22	636	2	-.0007	3T800K	6T800K
2278.3577	0 2 2 1 1	0 2 2 0 1	R	25D	636	2	.0000	3T800K	6T800K
2278.5368	0 1 1 1 1	0 1 1 0 1	R	8D	636	2	.0003	3T800K	
2278.7137	0 0 0 1 1	0 0 0 0 1	P	6	636	2	-.0024	3T800K	6T800K
2278.8996	0 0 0 1 1	0 0 0 0 1	R	18	638	2	.0003	3T800K	6T800K
2278.9833	0 2 2 1 1	0 2 2 0 1	R	26C	636	2	-.0001	6T800K	3T800K
2279.1163	1 0 0 1 1	1 0 0 0 1	R	22	636	2	-.0008	6T800K	3T800K
2279.2496	0 1 1 1 1	0 1 1 0 1	R	9C	636	2	-.0001	3T800K	
2279.5241	0 0 0 1 1	0 0 0 0 1	R	19	638	2	.0005	6T800K	3T800K
2279.5755	1 0 0 1 2	1 0 0 0 2	R	24	636	2	.0010	6T800K	3T800K
2279.6003	0 2 2 1 1	0 2 2 0 1	R	27D	636	2	-.0008	3T800K	
2279.9769	0 1 1 1 1	0 1 1 0 1	R	10D	636	2	-.0003	3T800K	
2280.1410	0 0 0 1 1	0 0 0 0 1	R	20	638	2	-.0012	3T800K	6T800K
2280.2153	0 2 2 1 1	0 2 2 0 1	R	28C	636	2	.0000	6T800K	3T800K
2280.3808	1 0 0 1 1	1 0 0 0 1	R	24	636	2	-.0002	3T800K	
2280.6771	0 1 1 1 1	0 1 1 0 1	R	11C	636	2	.0002	3T800K	
2280.7549	0 0 0 1 1	0 0 0 0 1	R	21	638	2	-.0002	3T800K	6T800K
2281.3622	0 0 0 1 1	0 0 0 0 1	R	22	638	2	-.0002	3T800K	
2281.3944	0 1 1 1 1	0 1 1 0 1	R	12D	636	2	.0002	3T800K	
2281.4228	0 2 2 1 1	0 2 2 0 1	R	30C	636	2	-.0007	3T800K	6T800K
2281.6191	1 0 0 1 1	1 0 0 0 1	R	26	636	2	-.0015	3T800K	6T800K
2281.9200	0 0 0 1 1	0 0 0 0 1	P	2	636	2	-.0008	3T800K	
2281.9640	0 0 0 1 1	0 0 0 0 1	R	23	638	2	-.0001	3T800K	
2282.0175	0 2 2 1 1	0 2 2 0 1	R	31D	636	2	.0005	3T800K	6T800K
2282.0648	1 0 0 1 2	1 0 0 0 2	R	28	636	2	.0018	3T800K	
2282.0799	0 1 1 1 1	0 1 1 0 1	R	13C	636	2	-.0006	3T800K	
2282.5597	0 0 0 1 1	0 0 0 0 1	R	24	638	2	-.0004	6T800K	3T800K
2282.6081	0 2 2 1 1	0 2 2 0 1	R	32C	636	2	.0001	3T800K	6T800K
2282.7868	0 1 1 1 1	0 1 1 0 1	R	14D	636	2	-.0005	3T800K	
2282.8376	1 0 0 1 1	1 0 0 0 1	R	28	636	2	.0016	6T800K	3T800K
2283.1509	0 0 0 1 1	0 0 0 0 1	R	25	638	2	.0004	3T800K	6T800K
2283.1898	0 2 2 1 1	0 2 2 0 1	R	33D	636	2	.0004	3T800K	6T800K
2283.2722	1 0 0 1 2	1 0 0 0 2	R	30	636	2	.0001	3T800K	6T800K
2283.4597	0 1 1 1 1	0 1 1 0 1	R	15C	636	2	-.0007	3T800K	
2283.7355	0 0 0 1 1	0 0 0 0 1	R	26	638	2	.0003	3T800K	
2283.7690	0 2 2 1 1	0 2 2 0 1	R	34C	636	2	.0001	3T800K	6T800K
2284.0276	1 0 0 1 1	1 0 0 0 1	R	30	636	2	.0005	6T800K	3T800K
2284.1563	0 1 1 1 1	0 1 1 0 1	R	16D	636	2	-.0004	3T800K	6T800K
2284.2616	0 0 0 1 1	0 0 0 0 1	R	0	636	2	-.0006	3T800K	
2284.3145	0 0 0 1 1	0 0 0 0 1	R	27	638	2	.0002	3T800K	6T800K
2284.3381	0 2 2 1 1	0 2 2 0 1	R	35D	636	2	.0000	3T800K	
2284.4581	1 0 0 1 2	1 0 0 0 2	R	32	636	2	.0003	6T800K	3T800K
2284.8173	0 1 1 1 1	0 1 1 0 1	R	17C	636	2	.0005	3T800K	
2284.8885	0 0 0 1 1	0 0 0 0 1	R	28	638	2	.0008	3T800K	6T800K
2284.9040	0 2 2 1 1	0 2 2 0 1	R	36C	636	2	-.0021	3T800K	

2285.1940	1 0 0 1 1	1 0 0 0 1	R	32	636	2	.0001	3T800K	6T800K
2285.5020	0 1 1 1 1	0 1 1 0 1	R	18D	636	2	-.0002	3T800K	
2285.6196	1 0 0 1 2	1 0 0 0 2	R	34	636	2	-.0003	3T800K	6T800K
2285.7937	0 0 0 1 1	0 0 0 0 1	R	2	636	2	.0002	3T800K	
2286.0186	0 0 0 1 1	0 0 0 0 1	R	30	638	2	.0010	3T800K	6T800K
2286.0187	0 2 2 1 1	0 2 2 0 1	R	38C	636	2	-.0008	6T800K	3T800K
2286.1494	0 1 1 1 1	0 1 1 0 1	R	19C	636	2	.0000	3T800K	
2286.3375	1 0 0 1 1	1 0 0 0 1	R	34	636	2	.0011	6T800K	3T800K
2286.7589	1 0 0 1 2	1 0 0 0 2	R	36	636	2	.0004	3T800K	6T800K
2286.8232	0 1 1 1 1	0 1 1 0 1	R	20D	636	2	-.0007	3T800K	
2287.1225	0 0 0 1 1	0 0 0 0 1	R	32	638	2	-.0023	3T800K	
2287.2995	0 0 0 1 1	0 0 0 0 1	R	4	636	2	-.0016	3T800K	
2287.4585	0 1 1 1 1	0 1 1 0 1	R	21C	636	2	.0001	3T800K	
2287.6415	0 2 2 1 1	0 2 2 0 1	R	41D	636	2	.0000	6T800K	3T800K
2287.6699	0 0 0 1 1	0 0 0 0 1	R	33	638	2	.0000	3T800K	6T800K
2287.8736	1 0 0 1 2	1 0 0 0 2	R	38	636	2	.0001	3T800K	6T800K
2288.1214	0 1 1 1 1	0 1 1 0 1	R	22D	636	2	-.0004	3T800K	
2288.1754	0 2 2 1 1	0 2 2 0 1	R	42C	636	2	.0002	3T800K	6T800K
2288.2094	0 0 0 1 1	0 0 0 0 1	R	34	638	2	.0001	6T800K	3T800K
2288.5483	1 0 0 1 1	1 0 0 0 1	R	38	636	2	-.0001	3T800K	
2288.6951	0 2 2 1 1	0 2 2 0 1	R	43D	636	2	.0000	3T800K	6T800K
2288.7437	0 0 0 1 1	0 0 0 0 1	R	35	638	2	.0007	3T800K	
2288.7437	0 1 1 1 1	0 1 1 0 1	R	23C	636	2	.0001	3T800K	
2288.7831	0 0 0 1 1	0 0 0 0 1	R	6	636	2	-.0017	3T800K	
2288.9651	1 0 0 1 2	1 0 0 0 2	R	40	636	2	.0001	3T800K	6T800K
2289.2173	0 2 2 1 1	0 2 2 0 1	R	44C	636	2	-.0002	3T800K	6T800K
2289.2713	0 0 0 1 1	0 0 0 0 1	R	36	638	2	.0002	6T800K	3T800K
2289.3958	0 1 1 1 1	0 1 1 0 1	R	24D	636	2	.0001	3T800K	
2289.6180	1 0 0 1 1	1 0 0 0 1	R	40	636	2	.0002	3T800K	
2289.7247	0 2 2 1 1	0 2 2 0 1	R	45D	636	2	-.0001	3T800K	6T800K
2289.7935	0 0 0 1 1	0 0 0 0 1	R	37	638	2	.0000	3T800K	6T800K
2290.0055	0 1 1 1 1	0 1 1 0 1	R	25C	636	2	.0004	3T800K	
2290.0323	1 0 0 1 2	1 0 0 0 2	R	42	636	2	-.0006	3T800K	
2290.2365	0 2 2 1 1	0 2 2 0 1	R	46C	636	2	.0006	6T800K	
2290.2428	0 0 0 1 1	0 0 0 0 1	R	8	636	2	-.0020	3T800K	
2290.3108	0 0 0 1 1	0 0 0 0 1	R	38	638	2	.0006	6T800K	3T800K
2290.6458	0 1 1 1 1	0 1 1 0 1	R	26D	636	2	.0001	3T800K	
2290.7306	0 2 2 1 1	0 2 2 0 1	R	47D	636	2	.0000	3T800K	6T800K
2290.8214	0 0 0 1 1	0 0 0 0 1	R	39	638	2	.0002	3T800K	6T800K
2291.0769	1 0 0 1 2	1 0 0 0 2	R	44	636	2	-.0002	6T800K	3T800K
2291.3267	0 0 0 1 1	0 0 0 0 1	R	40	638	2	.0001	6T800K	3T800K
2291.6829	1 0 0 1 1	1 0 0 0 1	R	44	636	2	-.0007	3T800K	
2291.7105	0 2 2 1 1	0 2 2 0 1	R	49D	636	2	-.0021	3T800K	
2291.8264	0 0 0 1 1	0 0 0 0 1	R	41	638	2	.0002	3T800K	6T800K
2291.8716	0 1 1 1 1	0 1 1 0 1	R	28D	636	2	-.0001	3T800K	
2292.0976	1 0 0 1 2	1 0 0 0 2	R	46	636	2	-.0001	3T800K	
2292.2010	0 2 2 1 1	0 2 2 0 1	R	50C	636	2	-.0003	6T800K	3T800K
2292.3202	0 0 0 1 1	0 0 0 0 1	R	42	638	2	.0000	6T800K	3T800K
2292.4571	0 1 1 1 1	0 1 1 0 1	R	29C	636	2	.0004	3T800K	
2292.8091	0 0 0 1 1	0 0 0 0 1	R	43	638	2	.0007	3T800K	6T800K

2293.1485	0	2	2	1	1	0	2	2	0	1	R	52C	636	2	.0002	3T800K	
2293.2903	0	0	0	1	1	0	0	0	0	1	R	44	638	2	-.0007	6T800K	3T800K
2293.6049	0	2	2	1	1	0	2	2	0	1	R	53D	636	2	.0000	6T800K	3T800K
2293.6469	0	1	1	1	1	0	1	1	0	1	R	31C	636	2	.0000	3T800K	
2293.7677	0	0	0	1	1	0	0	0	0	1	R	45	638	2	-.0001	3T800K	6T800K
2294.0686	1	0	0	1	2	1	0	0	0	2	R	50	636	2	.0007	6T800K	3T800K
2294.0688	0	2	2	1	1	0	2	2	0	1	R	54C	636	2	-.0026	3T800K	
2294.4793	0	0	0	1	1	0	0	0	0	1	R	14	636	2	-.0023	3T800K	
2294.5985	1	0	0	1	1	1	0	0	0	1	R	50	636	2	-.0004	6T800K	3T800K
2294.7041	0	0	0	1	1	0	0	0	0	1	R	47	638	2	-.0003	3T800K	
2294.8129	0	1	1	1	1	0	1	1	0	1	R	33C	636	2	-.0003	3T800K	
2294.9712	0	2	2	1	1	0	2	2	0	1	R	56C	636	2	.0005	3T800K	6T800K
2295.0171	1	0	0	1	2	1	0	0	0	2	R	52	636	2	-.0003	3T800K	6T800K
2295.1644	0	0	0	1	1	0	0	0	0	1	R	48	638	2	.0002	6T800K	3T800K
2295.4055	0	1	1	1	1	0	1	1	0	1	R	34D	636	2	-.0005	3T800K	
2295.5218	1	0	0	1	1	1	0	0	0	1	R	52	636	2	.0000	3T800K	6T800K
2295.6181	0	0	0	1	1	0	0	0	0	1	R	49	638	2	-.0001	6T800K	3T800K
2295.8478	0	0	0	1	1	0	0	0	0	1	R	16	636	2	.0017	6T800K	
2295.8478	0	2	2	1	1	0	2	2	0	1	R	58C	636	2	.0017	3T800K	6T800K
2295.9546	0	1	1	1	1	0	1	1	0	1	R	35C	636	2	-.0010	3T800K	6T800K
2296.0642	0	0	0	1	1	0	0	0	0	1	R	50	638	2	-.0023	3T800K	
2296.2638	0	2	2	1	1	0	2	2	0	1	R	59D	636	2	.0000	3T800K	
2296.4199	1	0	0	1	1	1	0	0	0	1	R	54	636	2	-.0002	6T800K	3T800K
2296.5101	0	0	0	1	1	0	0	0	0	1	R	51	638	2	.0009	6T800K	3T800K
2296.5360	0	1	1	1	1	0	1	1	0	1	R	36D	636	2	.0000	3T800K	6T800K
2296.6979	0	2	2	1	1	0	2	2	0	1	R	60C	636	2	.0002	3T800K	6T800K
2296.8445	1	0	0	1	2	1	0	0	0	2	R	56	636	2	-.0006	3T800K	6T800K
2296.9465	0	0	0	1	1	0	0	0	0	1	R	52	638	2	.0005	6T800K	3T800K
2297.0745	0	1	1	1	1	0	1	1	0	1	R	37C	636	2	.0003	3T800K	
2297.1017	0	2	2	1	1	0	2	2	0	1	R	61D	636	2	-.0005	3T800K	
2297.1854	0	0	0	1	1	0	0	0	0	1	R	18	636	2	-.0013	3T800K	
2297.2937	1	0	0	1	1	1	0	0	0	1	R	56	636	2	-.0002	3T800K	6T800K
2297.3775	0	0	0	1	1	0	0	0	0	1	R	53	638	2	.0003	3T800K	6T800K
2297.5253	0	2	2	1	1	0	2	2	0	1	R	62C	636	2	.0000	6T800K	3T800K
2297.6424	0	1	1	1	1	0	1	1	0	1	R	38D	636	2	.0004	3T800K	
2297.7227	1	0	0	1	2	1	0	0	0	2	R	58	636	2	-.0006	6T800K	3T800K
2297.8031	0	0	0	1	1	0	0	0	0	1	R	54	638	2	.0004	3T800K	6T800K
2297.9165	0	2	2	1	1	0	2	2	0	1	R	63D	636	2	.0000	3T800K	6T800K
2298.1446	1	0	0	1	1	1	0	0	0	1	R	58	636	2	.0014	3T800K	6T800K
2298.1689	0	1	1	1	1	0	1	1	0	1	R	39C	636	2	.0000	3T800K	
2298.2219	0	0	0	1	1	0	0	0	0	1	R	55	638	2	-.0005	3T800K	6T800K
2298.3293	0	2	2	1	1	0	2	2	0	1	R	64C	636	2	.0003	6T800K	3T800K
2298.5030	0	0	0	1	1	0	0	0	0	1	R	20	636	2	-.0003	3T800K	6T800K
2298.5768	1	0	0	1	2	1	0	0	0	2	R	60	636	2	-.0008	3T800K	6T800K
2298.6362	0	0	0	1	1	0	0	0	0	1	R	56	638	2	-.0002	3T800K	6T800K
2298.7238	0	1	1	1	1	0	1	1	0	1	R	40D	636	2	-.0001	3T800K	
2298.9693	1	0	0	1	1	1	0	0	0	1	R	60	636	2	.0014	6T800K	3T800K
2299.0444	0	0	0	1	1	0	0	0	0	1	R	57	638	2	-.0003	6T800K	3T800K
2299.1097	0	2	2	1	1	0	2	2	0	1	R	66C	636	2	.0008	6T800K	3T800K
2299.2394	0	1	1	1	1	0	1	1	0	1	R	41C	636	2	-.0002	3T800K	6T800K

2299.4075	1 0 0 1 2	1 0 0 0 2	R 62	636	2	-.0006	3T800K	6T800K
2299.4472	0 0 0 1 1	0 0 0 0 1	R 58	638	2	.0000	6T800K	3T800K
2299.4731	0 2 2 1 1	0 2 2 0 1	R 67D	636	2	-.0001	3T800K	6T800K
2299.7948	0 0 0 1 1	0 0 0 0 1	R 22	636	2	-.0012	6T800K	
2299.8433	0 0 0 1 1	0 0 0 0 1	R 59	638	2	-.0007	3T800K	
2299.8646	0 2 2 1 1	0 2 2 0 1	R 68C	636	2	-.0001	3T800K	
2300.2154	0 2 2 1 1	0 2 2 0 1	R 69D	636	2	-.0001	3T800K	
2300.2154	1 0 0 1 2	1 0 0 0 2	R 64	636	2	.0006	3T800K	6T800K
2300.2342	0 0 0 1 1	0 0 0 0 1	R 60	638	2	-.0009	6T800K	3T800K
2300.2865	0 1 1 1 1	0 1 1 0 1	R 43C	636	2	.0001	3T800K	
2300.5435	1 0 0 1 1	1 0 0 0 1	R 64	636	2	-.0002	6T800K	3T800K
2300.5941	0 2 2 1 1	0 2 2 0 1	R 70C	636	2	-.0026	3T800K	6T800K
2300.6206	0 0 0 1 1	0 0 0 0 1	R 61	638	2	.0002	6T800K	3T800K
2300.8155	0 1 1 1 1	0 1 1 0 1	R 44D	636	2	.0002	3T800K	
2300.9339	0 2 2 1 1	0 2 2 0 1	R 71D	636	2	.0002	3T800K	
2300.9984	0 0 0 1 1	0 0 0 0 1	R 62	638	2	-.0016	6T800K	3T800K
2300.9984	1 0 0 1 2	1 0 0 0 2	R 66	636	2	.0009	3T800K	6T800K
2301.0632	0 0 0 1 1	0 0 0 0 1	R 24	636	2	-.0014	3T800K	
2301.3092	0 1 1 1 1	0 1 1 0 1	R 45C	636	2	-.0001	3T800K	6T800K
2301.3734	0 0 0 1 1	0 0 0 0 1	R 63	638	2	-.0004	6T800K	3T800K
2301.6278	0 2 2 1 1	0 2 2 0 1	R 73D	636	2	.0000	6T800K	3T800K
2301.7437	0 0 0 1 1	0 0 0 0 1	R 64	638	2	.0018	6T800K	
2301.8245	0 1 1 1 1	0 1 1 0 1	R 46D	636	2	-.0003	3T800K	6T800K
2301.9877	0 2 2 1 1	0 2 2 0 1	R 74C	636	2	-.0011	3T800K	6T800K
2302.0212	1 0 0 1 1	1 0 0 0 1	R 68	636	2	.0003	6T800K	
2302.1041	0 0 0 1 1	0 0 0 0 1	R 65	638	2	-.0001	6T800K	3T800K
2302.2974	0 2 2 1 1	0 2 2 0 1	R 75D	636	2	-.0004	6T800K	
2302.3091	0 0 0 1 1	0 0 0 0 1	R 26	636	2	-.0002	3T800K	
2302.3091	0 1 1 1 1	0 1 1 0 1	R 47C	636	2	.0009	3T800K	
2302.4610	0 0 0 1 1	0 0 0 0 1	R 66	638	2	.0002	3T800K	6T800K
2302.4901	1 0 0 1 2	1 0 0 0 2	R 70	636	2	-.0012	6T800K	3T800K
2302.6508	0 2 2 1 1	0 2 2 0 1	R 76C	636	2	.0019	6T800K	3T800K
2302.7222	1 0 0 1 1	1 0 0 0 1	R 70	636	2	-.0004	6T800K	3T800K
2302.8105	0 0 0 1 1	0 0 0 0 1	R 67	638	2	-.0012	6T800K	3T800K
2302.8105	0 1 1 1 1	0 1 1 0 1	R 48D	636	2	.0004	3T800K	6T800K
2302.9440	0 2 2 1 1	0 2 2 0 1	R 77D	636	2	.0003	6T800K	3T800K
2303.1545	0 0 0 1 1	0 0 0 0 1	R 68	638	2	-.0023	3T800K	
2303.2013	1 0 0 1 2	1 0 0 0 2	R 72	636	2	-.0009	3T800K	6T800K
2303.2830	0 1 1 1 1	0 1 1 0 1	R 49C	636	2	-.0001	3T800K	6T800K
2303.2830	0 2 2 1 1	0 2 2 0 1	R 78C	636	2	-.0021	3T800K	6T800K
2303.3993	1 0 0 1 1	1 0 0 0 1	R 72	636	2	-.0004	3T800K	
2303.4985	0 0 0 1 1	0 0 0 0 1	R 69	638	2	.0024	3T800K	
2303.5303	0 0 0 1 1	0 0 0 0 1	R 28	636	2	.0004	3T800K	
2303.7713	0 1 1 1 1	0 1 1 0 1	R 50D	636	2	.0001	3T800K	6T800K
2303.8300	0 0 0 1 1	0 0 0 0 1	R 70	638	2	.0003	3T800K	
2303.8909	1 0 0 1 2	1 0 0 0 2	R 74	636	2	.0017	6T800K	3T800K
2304.0518	1 0 0 1 1	1 0 0 0 1	R 74	636	2	-.0002	6T800K	
2304.1598	0 0 0 1 1	0 0 0 0 1	R 71	638	2	.0023	3T800K	6T800K
2304.2343	0 1 1 1 1	0 1 1 0 1	R 51C	636	2	.0003	3T800K	
2304.4820	0 0 0 1 1	0 0 0 0 1	R 72	638	2	.0025	3T800K	

2304.5523	1	0	0	1	2	1	0	0	0	2	R	76	636	2	.0002	3T800K	
2304.6816	1	0	0	1	1	1	0	0	0	1	R	76	636	2	.0019	3T800K	
2304.7256	0	0	0	1	1	0	0	0	0	1	R	30	636	2	-.0008	3T800K	
2304.7980	0	0	0	1	1	0	0	0	0	1	R	73	638	2	.0022	3T800K	6T800K
2305.0505	0	2	2	1	1	0	2	2	0	1	R	84C	636	2	.0007	3T800K	6T800K
2305.1064	0	0	0	1	1	0	0	0	0	1	R	74	638	2	.0001	6T800K	3T800K
2305.1612	0	1	1	1	1	0	1	1	0	1	R	53C	636	2	.0004	3T800K	
2305.1918	1	0	0	1	2	1	0	0	0	2	R	78	636	2	.0007	3T800K	
2305.2834	0	2	2	1	1	0	2	2	0	1	R	85D	636	2	-.0025	3T800K	
2305.2834	1	0	0	1	1	1	0	0	0	1	R	78	636	2	.0008	3T800K	6T800K
2305.4111	0	0	0	1	1	0	0	0	0	1	R	75	638	2	.0001	6T800K	3T800K
2305.5916	0	2	2	1	1	0	2	2	0	1	R	86C	636	2	.0015	3T800K	6T800K
2305.6208	0	1	1	1	1	0	1	1	0	1	R	54D	636	2	.0000	3T800K	6T800K
2305.7099	0	0	0	1	1	0	0	0	0	1	R	76	638	2	-.0001	6T800K	3T800K
2305.8076	1	0	0	1	2	1	0	0	0	2	R	80	636	2	.0016	3T800K	6T800K
2305.8618	1	0	0	1	1	1	0	0	0	1	R	80	636	2	.0010	3T800K	
2305.8970	0	0	0	1	1	0	0	0	0	1	R	32	636	2	-.0019	3T800K	
2306.0037	0	0	0	1	1	0	0	0	0	1	R	77	638	2	.0005	3T800K	6T800K
2306.0638	0	1	1	1	1	0	1	1	0	1	R	55C	636	2	.0002	6T800K	3T800K
2306.1062	0	2	2	1	1	0	2	2	0	1	R	88C	636	2	-.0002	6T800K	
2306.2908	0	0	0	1	1	0	0	0	0	1	R	78	638	2	.0002	3T800K	
2306.3125	0	2	2	1	1	0	2	2	0	1	R	89D	636	2	.0005	6T800K	
2306.3977	1	0	0	1	2	1	0	0	0	2	R	82	636	2	.0009	3T800K	6T800K
2306.4151	1	0	0	1	1	1	0	0	0	1	R	82	636	2	.0008	3T800K	
2306.5091	0	1	1	1	1	0	1	1	0	1	R	56D	636	2	-.0001	3T800K	6T800K
2306.5722	0	0	0	1	1	0	0	0	0	1	R	79	638	2	.0000	6T800K	3T800K
2306.7899	0	2	2	1	1	0	2	2	0	1	R	91D	636	2	.0012	6T800K	3T800K
2306.8482	0	0	0	1	1	0	0	0	0	1	R	80	638	2	.0002	3T800K	6T800K
2306.9420	1	0	0	1	1	1	0	0	0	1	R	84	636	2	-.0011	3T800K	6T800K
2306.9420	0	1	1	1	1	0	1	1	0	1	R	57C	636	2	-.0003	3T800K	6T800K
2307.0445	0	0	0	1	1	0	0	0	0	1	R	34	636	2	-.0027	3T800K	
2307.1169	0	0	0	1	1	0	0	0	0	1	R	81	638	2	-.0012	3T800K	
2307.2407	0	2	2	1	1	0	2	2	0	1	R	93D	636	2	-.0006	3T800K	6T800K
2307.3741	0	1	1	1	1	0	1	1	0	1	R	58D	636	2	.0008	6T800K	3T800K
2307.4459	1	0	0	1	1	1	0	0	0	1	R	86	636	2	-.0011	6T800K	3T800K
2307.5090	1	0	0	1	2	1	0	0	0	2	R	86	636	2	.0028	6T800K	
2307.5093	0	2	2	1	1	0	2	2	0	1	R	94C	636	2	-.0024	3T800K	6T800K
2307.7974	0	1	1	1	1	0	1	1	0	1	R	59C	636	2	.0005	3T800K	6T800K
2307.8938	0	0	0	1	1	0	0	0	0	1	R	84	638	2	.0003	6T800K	3T800K
2307.9273	1	0	0	1	1	1	0	0	0	1	R	88	636	2	.0011	3T800K	6T800K
2308.0242	1	0	0	1	2	1	0	0	0	2	R	88	636	2	-.0005	3T800K	
2308.1703	0	0	0	1	1	0	0	0	0	1	R	36	636	2	-.0011	3T800K	
2308.2132	0	1	1	1	1	0	1	1	0	1	R	60D	636	2	.0002	3T800K	6T800K
2308.3285	0	2	2	1	1	0	2	2	0	1	R	98C	636	2	-.0002	6T800K	
2308.3808	0	0	0	1	1	0	0	0	0	1	R	86	638	2	-.0007	6T800K	3T800K
2308.3808	1	0	0	1	1	1	0	0	0	1	R	90	636	2	.0002	6T800K	3T800K
2308.4544	0	2	2	1	1	0	2	2	0	1	R	99D	636	2	.0010	6T800K	
2308.5189	1	0	0	1	2	1	0	0	0	2	R	90	636	2	-.0002	3T800K	
2308.6268	0	1	1	1	1	0	1	1	0	1	R	61C	636	2	-.0007	3T800K	6T800K
2308.7022	0	2	2	1	1	0	2	2	0	1	R	100C	636	2	.0009	6T800K	

2308.8081	1	0	0	1	1	1	0	0	0	1	R 92	636	2	-.0020	3T800K	6T800K
2308.8081	0	2	2	1	1	0	2	2	0	1	R101D	636	2	-.0009	3T800K	
2308.8466	0	0	0	1	1	0	0	0	0	1	R 88	638	2	.0003	3T800K	
2308.9891	1	0	0	1	2	1	0	0	0	2	R 92	636	2	-.0002	3T800K	6T800K
2309.0284	0	1	1	1	1	0	1	1	0	1	R 62D	636	2	-.0001	6T800K	3T800K
2309.0701	0	0	0	1	1	0	0	0	0	1	R 89	638	2	.0001	3T800K	6T800K
2309.1433	0	2	2	1	1	0	2	2	0	1	R103D	636	2	.0031	6T800K	
2309.2149	1	0	0	1	1	1	0	0	0	1	R 94	636	2	.0001	3T800K	
2309.2705	0	0	0	1	1	0	0	0	0	1	R 38	636	2	-.0010	3T800K	
2309.3744	0	2	2	1	1	0	2	2	0	1	R104C	636	2	-.0003	6T800K	3T800K
2309.4339	0	1	1	1	1	0	1	1	0	1	R 63C	636	2	.0000	3T800K	6T800K
2309.4339	1	0	0	1	2	1	0	0	0	2	R 94	636	2	-.0014	3T800K	6T800K
2309.4997	0	0	0	1	1	0	0	0	0	1	R 91	638	2	-.0003	3T800K	6T800K
2309.5961	1	0	0	1	1	1	0	0	0	1	R 96	636	2	.0014	3T800K	6T800K
2309.7049	0	0	0	1	1	0	0	0	0	1	R 92	638	2	-.0014	6T800K	3T800K
2309.8188	0	1	1	1	1	0	1	1	0	1	R 64D	636	2	-.0008	6T800K	3T800K
2309.8572	1	0	0	1	2	1	0	0	0	2	R 96	636	2	.0001	6T800K	3T800K
2309.9067	0	0	0	1	1	0	0	0	0	1	R 93	638	2	.0000	6T800K	
2309.9491	1	0	0	1	1	1	0	0	0	1	R 98	636	2	-.0006	3T800K	6T800K
2310.2155	0	1	1	1	1	0	1	1	0	1	R 65C	636	2	-.0006	3T800K	6T800K
2310.2557	1	0	0	1	2	1	0	0	0	2	R 98	636	2	.0011	6T800K	3T800K
2310.2901	0	0	0	1	1	0	0	0	0	1	R 95	638	2	-.0001	3T800K	6T800K
2310.3465	0	0	0	1	1	0	0	0	0	1	R 40	636	2	-.0008	3T800K	
2310.4743	0	0	0	1	1	0	0	0	0	1	R 96	638	2	.0011	6T800K	3T800K
2310.5863	0	1	1	1	1	0	1	1	0	1	R 66D	636	2	.0000	3T800K	6T800K
2310.6290	1	0	0	1	2	1	0	0	0	2	R100	636	2	.0011	6T800K	
2310.6499	0	0	0	1	1	0	0	0	0	1	R 97	638	2	-.0005	6T800K	
2310.8228	0	0	0	1	1	0	0	0	0	1	R 98	638	2	.0010	6T800K	
2310.9745	0	1	1	1	1	0	1	1	0	1	R 67C	636	2	.0003	6T800K	3T800K
2310.9747	1	0	0	1	2	1	0	0	0	2	R102	636	2	-.0023	3T800K	
2311.1475	0	0	0	1	1	0	0	0	0	1	R100	638	2	.0004	6T800K	
2311.3032	1	0	0	1	2	1	0	0	0	2	R104	636	2	.0015	3T800K	
2311.3285	0	1	1	1	1	0	1	1	0	1	R 68D	636	2	-.0001	3T800K	6T800K
2311.3986	0	0	0	1	1	0	0	0	0	1	R 42	636	2	-.0004	3T800K	
2311.7081	0	1	1	1	1	0	1	1	0	1	R 69C	636	2	.0000	6T800K	3T800K
2312.0465	0	1	1	1	1	0	1	1	0	1	R 70D	636	2	-.0001	6T800K	3T800K
2312.4256	0	0	0	1	1	0	0	0	0	1	R 44	636	2	-.0008	3T800K	
2312.7399	0	1	1	1	1	0	1	1	0	1	R 72D	636	2	-.0001	6T800K	3T800K
2313.1034	0	1	1	1	1	0	1	1	0	1	R 73C	636	2	.0001	3T800K	6T800K
2313.4296	0	0	0	1	1	0	0	0	0	1	R 46	636	2	.0000	3T800K	
2313.7648	0	1	1	1	1	0	1	1	0	1	R 75C	636	2	.0002	6T800K	3T800K
2314.0535	0	1	1	1	1	0	1	1	0	1	R 76D	636	2	-.0001	3T800K	6T800K
2314.4081	0	0	0	1	1	0	0	0	0	1	R 48	636	2	-.0005	3T800K	
2314.6736	0	1	1	1	1	0	1	1	0	1	R 78D	636	2	.0000	6T800K	3T800K
2315.0141	0	1	1	1	1	0	1	1	0	1	R 79C	636	2	-.0003	3T800K	
2315.3635	0	0	0	1	1	0	0	0	0	1	R 50	636	2	.0003	3T800K	
2315.6029	0	1	1	1	1	0	1	1	0	1	R 81C	636	2	.0000	6T800K	
2315.8402	0	1	1	1	1	0	1	1	0	1	R 82D	636	2	.0000	3T800K	6T800K
2316.1676	0	1	1	1	1	0	1	1	0	1	R 83C	636	2	.0005	3T800K	6T800K
2316.2930	0	0	0	1	1	0	0	0	0	1	R 52	636	2	-.0005	3T800K	

2316.3864	0	1	1	1	1	0	1	1	0	1	R 84D	636	2	-.0002	6T800K	3T800K
2316.7089	0	1	1	1	1	0	1	1	0	1	R 85C	636	2	-.0001	3T800K	6T800K
2316.9086	0	1	1	1	1	0	1	1	0	1	R 86D	636	2	.0002	6T800K	3T800K
2317.1987	0	0	0	1	1	0	0	0	0	1	R 54	636	2	-.0008	3T800K	
2317.4058	0	1	1	1	1	0	1	1	0	1	R 88D	636	2	.0001	6T800K	3T800K
2317.7124	0	1	1	1	1	0	1	1	0	1	R 89C	636	2	-.0015	6T800K	3T800K
2317.8783	0	1	1	1	1	0	1	1	0	1	R 90D	636	2	.0000	6T800K	3T800K
2318.0813	0	0	0	1	1	0	0	0	0	1	R 56	636	2	.0001	3T800K	
2318.1809	0	1	1	1	1	0	1	1	0	1	R 91C	636	2	.0001	6T800K	3T800K
2318.3267	0	1	1	1	1	0	1	1	0	1	R 92D	636	2	.0004	3T800K	6T800K
2318.6237	0	1	1	1	1	0	1	1	0	1	R 93C	636	2	.0004	6T800K	3T800K
2318.7494	0	1	1	1	1	0	1	1	0	1	R 94D	636	2	-.0003	6T800K	3T800K
2318.9387	0	0	0	1	1	0	0	0	0	1	R 58	636	2	.0002	3T800K	6T800K
2319.0413	0	1	1	1	1	0	1	1	0	1	R 95C	636	2	-.0002	3T800K	6T800K
2319.1489	0	1	1	1	1	0	1	1	0	1	R 96D	636	2	.0005	6T800K	3T800K
2319.4354	0	1	1	1	1	0	1	1	0	1	R 97C	636	2	.0001	6T800K	3T800K
2319.5222	0	1	1	1	1	0	1	1	0	1	R 98D	636	2	-.0002	3T800K	6T800K
2319.7714	0	0	0	1	1	0	0	0	0	1	R 60	636	2	.0001	3T800K	6T800K
2319.8639	0	1	1	1	1	0	1	1	0	1	R 99C	636	2	-.0007	3T800K	
2319.8719	0	1	1	1	1	0	1	1	0	1	R100D	636	2	.0003	6T800K	3T800K
2320.1500	0	1	1	1	1	0	1	1	0	1	R101C	636	2	.0004	6T800K	3T800K
2320.1960	0	1	1	1	1	0	1	1	0	1	R102D	636	2	-.0002	6T800K	3T800K
2320.4965	0	1	1	1	1	0	1	1	0	1	R104D	636	2	.0005	3T800K	6T800K
2320.5798	0	0	0	1	1	0	0	0	0	1	R 62	636	2	.0000	3T800K	
2320.7689	0	1	1	1	1	0	1	1	0	1	R106D	636	2	-.0021	3T800K	
2320.7689	0	1	1	1	1	0	1	1	0	1	R105C	636	2	.0027	3T800K	
2321.0201	0	1	1	1	1	0	1	1	0	1	R108D	636	2	-.0012	3T800K	6T800K
2321.0377	0	1	1	1	1	0	1	1	0	1	R107C	636	2	-.0002	6T800K	3T800K
2321.2467	0	1	1	1	1	0	1	1	0	1	R110D	636	2	.0000	6T800K	3T800K
2321.3636	0	0	0	1	1	0	0	0	0	1	R 64	636	2	-.0002	3T800K	
2321.4477	0	1	1	1	1	0	1	1	0	1	R112D	636	2	.0004	6T800K	
2322.1232	0	0	0	1	1	0	0	0	0	1	R 66	636	2	-.0002	3T800K	6T800K
2322.8587	0	0	0	1	1	0	0	0	0	1	R 68	636	2	.0002	6T800K	3T800K
2323.5691	0	0	0	1	1	0	0	0	0	1	R 70	636	2	.0000	3T800K	6T800K
2324.2555	0	0	0	1	1	0	0	0	0	1	R 72	636	2	.0003	3T800K	
2324.9169	0	0	0	1	1	0	0	0	0	1	R 74	636	2	.0002	6T800K	3T800K
2325.5537	0	0	0	1	1	0	0	0	0	1	R 76	636	2	.0000	6T800K	3T800K
2326.1663	0	0	0	1	1	0	0	0	0	1	R 78	636	2	.0002	3T800K	6T800K
2326.7540	0	0	0	1	1	0	0	0	0	1	R 80	636	2	.0000	6T800K	3T800K
2327.3174	0	0	0	1	1	0	0	0	0	1	R 82	636	2	.0002	3T800K	6T800K
2327.8558	0	0	0	1	1	0	0	0	0	1	R 84	636	2	.0000	6T800K	3T800K
2328.3700	0	0	0	1	1	0	0	0	0	1	R 86	636	2	.0003	6T800K	3T800K
2328.8590	0	0	0	1	1	0	0	0	0	1	R 88	636	2	.0001	6T800K	3T800K
2329.3240	0	0	0	1	1	0	0	0	0	1	R 90	636	2	.0005	3T800K	6T800K
2329.7634	0	0	0	1	1	0	0	0	0	1	R 92	636	2	.0000	6T800K	3T800K
2330.1794	0	0	0	1	1	0	0	0	0	1	R 94	636	2	.0009	3T800K	6T800K
2330.9340	0	0	0	1	1	0	0	0	0	1	R 98	636	2	-.0006	3T800K	
2331.2751	0	0	0	1	1	0	0	0	0	1	R100	636	2	-.0003	6T800K	3T800K
2331.5920	0	0	0	1	1	0	0	0	0	1	R102	636	2	.0005	6T800K	3T800K
2331.8831	0	0	0	1	1	0	0	0	0	1	R104	636	2	.0003	6T800K	3T800K

2332.1491	0	0	0	1	1	0	0	0	0	1	R106	636	2	-.0001	6T800K	3T800K
2332.3904	0	0	0	1	1	0	0	0	0	1	R108	636	2	-.0004	3T800K	
2332.6075	0	0	0	1	1	0	0	0	0	1	R110	636	2	.0000	6T800K	3T800K
2332.7992	0	0	0	1	1	0	0	0	0	1	R112	636	2	-.0001	6T800K	3T800K
2332.9661	0	0	0	1	1	0	0	0	0	1	R114	636	2	-.0002	6T800K	3T800K
2333.1085	0	0	0	1	1	0	0	0	0	1	R116	636	2	.0002	6T800K	
2333.2270	0	0	0	1	1	0	0	0	0	1	R118	636	2	.0016	6T800K	
2333.3186	0	0	0	1	1	0	0	0	0	1	R120	636	2	.0010	6T800K	
2333.3835	0	0	0	1	1	0	0	0	0	1	R122	636	2	-.0013	6T800K	

Table IX. H_2O Line Data Between 1600 cm^{-1} and 2000 cm^{-1}

The listings are:

the transition frequency in cm^{-1}

the absorption strength in cm^{-1}/molecule cm^{-2} at 800K

the integrated absorptance in cm^{-1} for the H_2O column density 2.17 x 10^{20} molecules/cm^2 at 800K

the lower state energy in cm^{-1}

the transition assignment in (J', K_a', K_c'), (J'', K_a'', K_c''), (v_1', v_2', v_3'), and (v_1'', v_2'', v_3'')

an internal code

the isotope code

the molecule identification code

the integrated absorptance in cm^{-1} for the H_2O column density 2.17 x 10^{20} molecules/cm^2 at 800K, and

the wavenumber difference between the measured and the one listed in the AFGL (1978) listing.

cannot fully legible reproduction

Copy furnished to DTIC does not permit fully legible reproduction

Table X.

Newly identified lines of the (010-000) and (020-010) bands.

Transition	Position
(010-000) band	
$21_{1,21} - 20_{0,20}$ } $21_{0,21} - 20_{1,20}$	1949.9147 cm^{-1}
$22_{1,22} - 21_{0,21}$ } $22_{0,22} - 21_{1,21}$	1963.4065
$23_{1,23} - 22_{0,22}$ } $23_{0,23} - 22_{1,22}$	1976.7223
$24_{1,24} - 23_{0,23}$ } $24_{0,24} - 23_{1,23}$	1989.9184
(020-010) band	
$12_{1,12} - 11_{0,11}$	1780.9916
$12_{0,12} - 11_{1,11}$	1780.9407
$13_{1,1}{}^{2} - 12_{2,1}$	1849.5795
$13_{1,13} - 12_{0,12}$	1797.0532
$13_{0,13} - 12_{1,12}$	1797.0276
$14_{1,13} - 13_{2112}$	1868.0298
$14_{1,14} - 13_{0,13}$	1812.8915 blended
$14_{0,14} - 13_{1,13}$	1812.8915
$15_{3,13} - 14_{2,12}$	1931.9649
$15_{2,13} - 14_{3,12}$	1928.6794
$15_{2,14} - 14_{1,13}$	1888.0332
$15_{1,14} - 14_{2,13}$	1887.7405

Table X. (Continued)

Transition	Position
$^{15}_{1,15} - {}^{14}_{0,14}$	1828.5181 cm^{-1}
$^{15}_{0,15} - {}^{14}_{1,14}$	1828.5127
$^{16}_{3,14} - {}^{15}_{2,13}$	1951.2771
$^{16}_{2,15} - {}^{15}_{1,14}$	1906.3849
$^{16}_{1,15} - {}^{15}_{2,14}$	1906.2534
$^{16}_{1,16} - {}^{15}_{0,15}$ } $^{16}_{0,16} - {}^{15}_{1,15}$	1843.9477
$^{17}_{1,17} - {}^{16}_{0,16}$ } $^{17}_{0,17} - {}^{16}_{1,16}$	1859.2010
$^{18}_{1,18} - {}^{17}_{0,17}$ } $^{18}_{0,18} - {}^{17}_{1,17}$	18 4.3132
$^{19}_{1,19} - {}^{18}_{0,18}$ } $^{19}_{0,19} - {}^{18}_{1,18}$	1889.3063
$^{20}_{1,20} - {}^{19}_{0,19}$ } $^{20}_{0,20} - {}^{19}_{1,19}$	1904.2398

References

1. W.S. Dalton and H. Sakai, App. Opt. 19, 2413 (1980).

2. H. Sakai, AFCRL-TR-0571 (1974), Air Force Geophysics Laboratory, Hanscom Air Force Base, MA 01731.

3. H. Sakai, "High-Resolving Power Fourier Spectroscopy," Spectrometric Techniques, Vol. I, G. Vanasse, Ed., Academic Press, New York (1977).

4. A.S. Pine and G. Guelachvili, J. Mol. Spectrosc. 79, 84 (1980).

5. G. Guelachvili, J. Mol. Spectrosc. 75, 251 (1979).

6. G. Herzberg, Spectra of Diatomic Molecules, Second Ed., p. 191, Van Nostrand Reinhold, New York (1950).

7. R.A. McClatchey, W.S. Benedict, S.A. Clough, D.E. Burch, R.F. Calfee, K. Fox, L.S. Rothman and J.S. Garing, AFCRL Report No. 434, 73-0096, p. 26 (1973).

8. L.S. Rothman, Appl. Opt. 17, 3517 (1978).

9. G. Guelachvili, J. Mol. Spectrosc. 79, 72 (1980).

10. L.S. Rothman and L.D. Young, JQSRT 25, 505 (1981).

11. L.S. Rothman, Appl. Opt. 20, 791 (1981).

12. M.P. Esplin and H. Sakai, Paper WP11, Topical Meeting on Spectroscopy in Support of Atmospheric Measurements, Sarasota, FL (1980); H. Sakai, Final Report on Grant AFOSR-78-3702 (1980), Astronomy Research Facility, University of Massachusetts, Amherst, MA 01003.

13. W.S. Benedict and L. Kaplan, JQSRT 4, 453 (1964); W.S. Benedict and L. Kaplan, J. Chem. Phys. 30, 388 (1959); R.W. Davies and B.A. Oli, JQSRT 20, 95 (1978).

14. A. Chedin, J. Mol. Spectrosc. 76, 430 (1979).

15. J.M. Brown, J.T. Hougen, K.P. Huber, J.W.C. Johns, I. Kopp, H. Lefebvre-Brion, A.J. Merer, D.A. Ramsay, J. Rostas, and R.N. Zare, J. Mol. Spectrosc. 55, 500 (1975).

16. R. Paso, J. Kauppinen, and R. Anttila, J. Mol. Spectrosc. 79, 236 (1980); R. Paso, U. Oulu, Finland, private communication.

17. C. Freed, L.C. Bradley, and R.G. O'Donnell, I.E.E.E. J.Q. Electronics 16, 1195 (1980).

18. J. Dupre-Maquaire and P. Pinson, J. Mol. Spectrosc. 62, 181 (1976).

19. K.J. Siemsen, Opt. Lett. 6, 114 (1981); K.J. Siemsen and B.G. Whitford, Opt. Comm. 22, 11 (1977); K.J. Siemsen, Opt. Comm. 34, 447 (1980); F.R. Petersen, J.S. Wells, A.G. Maki, and K.J. Siemsen, Appl. Opt. 20, 3635 (1981).

20. J.P. Maillard, J. Cuisenier, Ph. Arcas, E. Arie, and C. Amiot, Can. J. Phys. 58, 1560 (1980).

21. D. Bailly, R. Farrenq, G. Guelachvili, and C. Rosetti, J. Mol. Spectrosc. 90, 74 (1981); D. Bailly, Orsay, France, private communication.